

Nonlinear Fourier transform of time-limited and one-sided signals

Vaibhav, Vishal

DOI

[10.1088/1751-8121/aad9ab](https://doi.org/10.1088/1751-8121/aad9ab)

Publication date

2018

Document Version

Accepted author manuscript

Published in

Journal of Physics A: Mathematical and Theoretical

Citation (APA)

Vaibhav, V. (2018). Nonlinear Fourier transform of time-limited and one-sided signals. *Journal of Physics A: Mathematical and Theoretical*, 51(42), [425201]. <https://doi.org/10.1088/1751-8121/aad9ab>

Important note

To cite this publication, please use the final published version (if applicable).
Please check the document version above.

Copyright

Other than for strictly personal use, it is not permitted to download, forward or distribute the text or part of it, without the consent of the author(s) and/or copyright holder(s), unless the work is under an open content license such as Creative Commons.

Takedown policy

Please contact us and provide details if you believe this document breaches copyrights.
We will remove access to the work immediately and investigate your claim.

Nonlinear Fourier Transform of Time-Limited and One-sided Signals

Vishal Vaibhav*

(Dated: September 8, 2018)

In this article, we study the properties of the nonlinear Fourier spectrum in order to gain better control of the temporal support of the signals synthesized using the inverse nonlinear Fourier transform (NFT). In particular, we provide necessary and sufficient conditions satisfied by the nonlinear Fourier spectrum such that the generated signal has a prescribed support. In our exposition, we assume that the support is a simply connected domain that is either a bounded interval or the half-line, which amounts to studying the class of signals which are either time-limited or one-sided, respectively. Further, it is shown that the analyticity properties of the scattering coefficients of the aforementioned classes of signals can be exploited to improve the numerical conditioning of the differential approach of inverse scattering. Here, we also revisit the integral approach of inverse scattering and provide the correct derivation of the so called Töplitz inner-bordering algorithm. Finally, we conduct extensive numerical tests in order to verify the analytical results presented in the article. These tests also provide us an opportunity to compare the performance of the two aforementioned numerical approaches in terms of accuracy and complexity of computations.

Keywords: Nonlinear Fourier Transform, Layer-Peeling Algorithm, Töplitz Inner-Bordering Algorithm, Time-Limited Signals

NOTATIONS

The set of non-zero positive real numbers (\mathbb{R}) is denoted by \mathbb{R}_+ . Real and imaginary parts of complex numbers (\mathbb{C}) are denoted by $\text{Re}(\cdot)$ and $\text{Im}(\cdot)$, respectively. The complex conjugate of $\zeta \in \mathbb{C}$ is denoted by ζ^* . The upper half (lower half) of \mathbb{C} is denoted by \mathbb{C}_+ (\mathbb{C}_-) and its closure by $\overline{\mathbb{C}}_+$ ($\overline{\mathbb{C}}_-$). The support of a function $f : \Omega \rightarrow \mathbb{R}$ in Ω is defined as $\text{supp } f = \{x \in \Omega \mid f(x) \neq 0\}$. The Lebesgue spaces of complex-valued functions defined in \mathbb{R} are denoted by L^p for $1 \leq p \leq \infty$ with their corresponding norm denoted by $\|\cdot\|_{L^p}$ or $\|\cdot\|_p$. The inverse Fourier-Laplace transform of a function $F(\zeta)$ analytic in $\overline{\mathbb{C}}_+$ is defined as

$$f(\tau) = \frac{1}{2\pi} \int_{\Gamma} F(\zeta) e^{-i\zeta\tau} d\zeta,$$

where Γ is any contour parallel to the real line. The class of m -times differentiable complex-valued functions is denoted by C^m . A function of class C^m is said to belong to $C_0^m(\Omega)$, if the function and its derivatives up to order m have a compact support in Ω and if they vanish on the boundary ($\partial\Omega$).

I. INTRODUCTION

A nonlinear generalization of the conventional Fourier transform can be achieved via the two-component non-Hermitian Zakharov-Shabat (ZS) scattering problem [1]. As presented originally, it provides a means of solving certain nonlinear initial-value problems whose general description is provided by the AKNS-formalism [2, 3]. The role of the nonlinear Fourier transform (NFT) here is entirely analogous to that of the Fourier transform in solving linear initial-value problems (IVPs) of dispersive nature. One of the practical

applications of this theory is in optical fiber communication where the master equation for propagation of optical field in a loss-less single mode fiber under Kerr-type focusing nonlinearity is the nonlinear Schrödinger equation (NSE) [4, 5]:

$$i\partial_x q = \partial_t^2 q + 2|q|^2 q, \quad (t, x) \in \mathbb{R} \times \mathbb{R}_+, \quad (1)$$

where $q(t, x)$ is a complex valued function associated with the slowly varying envelope of the electric field, t is the retarded time and x is the position along the fiber. There is a growing interest in the research community to exploit the nonlinear Fourier spectrum of the optical pulses for encoding information in an attempt to mitigate nonlinear signal distortions at higher powers. This forms part of the motivation for this work where we study various signal processing aspects of NFT that may be useful in any NFT-based modulation scheme. We refer the reader to a comprehensive review article [6] and the references therein for an overview of NFT-based optical communication methodologies.

The ZS problem also appears naturally in certain physical systems. For instance, the coupled-mode equations for co-propagating modes in a grating-assisted co-directional coupler (GACC), a device used to couple light between two different guided modes of an optical fiber, is a ZS problem with the coupling coefficient as the potential (see [7, 8] and references therein). Note that the coupling coefficient of physical GACCs must be compactly supported. In [8], the consequence of this requirement was studied in a discrete framework.

In this work, we formulate the necessary and sufficient conditions for the nonlinear Fourier spectrum (continuous as well as discrete) such that the corresponding signal has a prescribed support. In addition, certain useful regularity properties of the continuous spectrum are proven which resemble that of the conventional Fourier transform. For the conventional Fourier transform, these results are already established in the well-known Paley-Wiener theorems. Note that a straightforward way of generating time-limited signals is by windowing using a rectangle function. In [9], exact solution of the scattering problem for a doubly-truncated multisoliton potential was presented. This task was accomplished by first solving for the

* vishal.vaibhav@gmail.com

one-sided potential obtained as a result of truncation from one side using the method discussed in the work of Lamb [10] (see also [11–13]). Both of these exactly solvable cases prove to be an insightful example of time-limited and one-sided signals where analyticity properties of the scattering coefficients can be determined precisely.

The next goal that we pursue in this work is to exploit these regularity properties to improve the numerical conditioning of the inverse scattering algorithms. In particular, we revisit the *differential approach* [14, 15] as well as the *integral approach* [16, 17] of inverse scattering, and, discuss how to synthesize the input to these algorithms such that the generated signal has the prescribed support. Further, we address in this work, the kind of numerical ill-conditioning that results from a pole of the reflection coefficient that is too ‘close’ to the real axis. It turns out that the analyticity property of the reflection coefficient, $\rho(\zeta)$, in \mathbb{C}_+ can be exploited to develop a robust inverse scattering algorithm within the differential approach that is based on the exponential *trapezoidal rule* presented in [14]. The advantage of the differential approach is also seen in other numerical examples in this article where the aforementioned second order convergent algorithm outperforms that based on the integral approach in terms of accuracy as well as complexity of computations.

The article is organized as follows: The main results of this paper for the continuous-time NFT is presented in Sec. II where we focus on certain class of time-limited and one-sided signals. In Sec. III, we discuss the two approaches for inverse scattering, namely, the differential and the integral approach. Sec. IV discusses all the numerical results and Sec. V concludes this article.

II. CONTINUOUS-TIME NONLINEAR FOURIER TRANSFORM

The starting point of our discussion is the ZS scattering problem for the complex-valued potentials $q(t, x)$ and $r(t, x) = -q^*(t, x)$ which in the AKNS-formalism (see [2] for a complete introduction) can be stated as follows: Let $\zeta \in \mathbb{R}$ and $\mathbf{v} = (v_1, v_2)^T$; then, for $t \in \mathbb{R}$,

$$\partial_t v_1 = -i\zeta v_1 + qv_2, \quad \partial_t v_2 = i\zeta v_2 + rv_1. \quad (2)$$

In this article, we are mostly interested in studying the NFT for a fixed x ; therefore, we suppress any dependence on x for the sake of brevity. The nonlinear Fourier spectrum can be defined using the scattering coefficients, namely, $a(\zeta)$ and $b(\zeta)$, which are determined from the asymptotic form of the Jost solution, $\mathbf{v} = \boldsymbol{\phi}(t; \zeta)$: As $t \rightarrow -\infty$, we have $\boldsymbol{\phi}e^{i\zeta t} \rightarrow (1, 0)^T$, and, as $t \rightarrow \infty$, we have $\boldsymbol{\phi} \rightarrow (a(\zeta)e^{-i\zeta t}, b(\zeta)e^{i\zeta t})^T$. An equivalent description of the system is obtained via the Jost solution $\mathbf{v} = \boldsymbol{\psi}(t; \zeta)$ whose asymptotic behavior as $t \rightarrow \infty$ is $\boldsymbol{\psi}(t; \zeta)e^{-i\zeta t} \rightarrow (0, 1)^T$, and, an equivalent set of scattering coefficients can be determined from its asymptotic form (as $t \rightarrow -\infty$) $\boldsymbol{\psi} \rightarrow (\bar{b}(\zeta)e^{-i\zeta t}, a(\zeta)e^{i\zeta t})^T$ with the symmetry property $\bar{b}(\zeta) = b^*(\zeta)$ ($\zeta \in \mathbb{R}$).

In general, the nonlinear Fourier spectrum for the potential $q(t)$ comprises a *discrete* and a *continuous spectrum*. The dis-

crete spectrum consists of the so called *eigenvalues* $\zeta_k \in \mathbb{C}_+$, such that $a(\zeta_k) = 0$, and, the *norming constants* b_k such that $\boldsymbol{\phi}(t; \zeta_k) = b_k \boldsymbol{\psi}(t; \zeta_k)$. Note that (ζ_k, b_k) describes a *bound state* or a *solitonic state* associated with the potential. For convenience, let the discrete spectrum be denoted by the set

$$\mathfrak{S}_K = \{(\zeta_k, b_k) \in \mathbb{C}^2 \mid \text{Im } \zeta_k > 0, k = 1, 2, \dots, K\}. \quad (3)$$

The continuous spectrum, also referred to as the *reflection coefficient*, is defined by $\rho(\xi) = b(\xi)/a(\xi)$ for $\xi \in \mathbb{R}$.

Introducing the ‘local’ scattering coefficients $a(t; \zeta)$ and $b(t; \zeta)$ such that $\boldsymbol{\phi}(t; \zeta) = (a(t; \zeta)e^{-i\zeta t}, b(t; \zeta)e^{i\zeta t})^T$, the scattering problem in (2) reads as

$$\begin{aligned} \partial_t a(t; \zeta) &= q(t)b(t; \zeta)e^{2i\zeta t}, \\ \partial_t b(t; \zeta) &= r(t)a(t; \zeta)e^{-2i\zeta t}. \end{aligned} \quad (4)$$

A. The direct transform: Time-limited signals

Let the scattering potential $q(t)$ be a time-limited signal with its support in $\Omega = [-T_-, T_+]$ where $T_{\pm} \geq 0$. The initial conditions for the Jost solution $\boldsymbol{\phi}$ are: $a(-T_-; \zeta) = 1$ and $b(-T_-; \zeta) = 0$. The scattering coefficients can be directly obtained from these functions as $a(\zeta) = a(T_+; \zeta)$ and $b(\zeta) = b(T_+; \zeta)$. For the type of potential at hand, these coefficients are known to be analytic functions of $\zeta \in \mathbb{C}$ [2].

In this section, it will be useful to transform the ZS problem in (4) as follows: Let us define, for the sake of convenience, the modified Jost solution

$$\tilde{\mathbf{P}}(t; \zeta) = \boldsymbol{\phi}(t; \zeta)e^{i\zeta t} - \begin{pmatrix} 1 \\ 0 \end{pmatrix} = \begin{pmatrix} a(t; \zeta) - 1 \\ b(t; \zeta)e^{2i\zeta t} \end{pmatrix}, \quad (5)$$

so that $\tilde{\mathbf{P}}(T_+; \zeta)e^{-2i\zeta T_+} = ([a(\zeta) - 1]e^{-2i\zeta T_+}, b(\zeta))^T$. The system of equations in (4) can be transformed into a set of Volterra integral equations of the second kind for $\tilde{\mathbf{P}}(t; \zeta)$:

$$\tilde{\mathbf{P}}(t; \zeta) = \boldsymbol{\Phi}(t; \zeta) + \int_{\Omega} \mathcal{K}(t, y; \zeta) \tilde{\mathbf{P}}(y; \zeta) dy, \quad (6)$$

where $\boldsymbol{\Phi}(t; \zeta) = (\Phi_1, \Phi_2)^T \in \mathbb{C}^2$ with

$$\begin{aligned} \Phi_1(t; \zeta) &= \int_{-T_-}^t q(z)\Phi_2(z; \zeta) dz, \\ \Phi_2(t; \zeta) &= \int_{-T_-}^t r(y)e^{2i\zeta(t-y)} dy, \end{aligned} \quad (7)$$

and the Volterra kernel $\mathcal{K}(x, y; \zeta) = \text{diag}(\mathcal{K}_1, \mathcal{K}_2) \in \mathbb{C}^{2 \times 2}$ is such that

$$\begin{aligned} \mathcal{K}_1(x, y; \zeta) &= r(y) \int_y^x q(z)e^{2i\zeta(z-y)} dz, \\ \mathcal{K}_2(x, y; \zeta) &= q(y) \int_y^x r(z)e^{2i\zeta(x-z)} dz, \end{aligned} \quad (8)$$

with $\mathcal{K}(x, y; \zeta) = 0$ for $y > x$. In the following, we establish that $a(\zeta)$ and $b(\zeta)$ are of exponential type in \mathbb{C} .

Theorem II.1. Let $q \in L^1$ with support in Ω and set $\kappa = \|q\|_{L^1(\Omega)}$. Then the estimates

$$|b(\zeta)| \leq \sinh(\kappa) \times \begin{cases} e^{2T_+ \operatorname{Im} \zeta}, & \zeta \in \overline{\mathbb{C}}_+, \\ e^{-2T_- \operatorname{Im} \zeta}, & \zeta \in \mathbb{C}_-, \end{cases} \quad (9)$$

$$|\tilde{a}(\zeta)| \leq [\cosh(\kappa) - 1] \times \begin{cases} e^{2T_+ \operatorname{Im} \zeta}, & \zeta \in \overline{\mathbb{C}}_+, \\ e^{-2T_- \operatorname{Im} \zeta}, & \zeta \in \mathbb{C}_-, \end{cases} \quad (10)$$

where $\tilde{a}(\zeta)$ denotes $[a(\zeta) - 1]e^{-2i\zeta T_+}$, hold. And, for fixed $\eta \in \mathbb{R}$ such that $|\eta| < \infty$, we have

$$\lim_{\xi \in \mathbb{R}, |\xi| \rightarrow \infty} |f(\xi + i\eta)| = 0, \quad (11)$$

where $f(\zeta)$ denotes either $b(\zeta)$ or $\tilde{a}(\zeta)$.

Proof. The proof can be obtained using the same method as in [2]. For fixed $\zeta \in \overline{\mathbb{C}}_+$, let \mathcal{K} denote the Volterra integral operator in (6) corresponding to the kernel $\mathcal{K}(x, y; \zeta)$ such that

$$\begin{aligned} \mathcal{K}[\tilde{\mathbf{P}}](t; \zeta) &= \int_{\Omega} \mathcal{K}(t, y; \zeta) \tilde{\mathbf{P}}(y; \zeta) dy \\ &= \int_{-T_-}^t dz \int_{-T_-}^z dy \begin{pmatrix} q(z)r(y)e^{2i\zeta(z-y)} \tilde{\mathbf{P}}_1(y; \zeta) \\ q(y)r(z)e^{2i\zeta(t-z)} \tilde{\mathbf{P}}_2(y; \zeta) \end{pmatrix}. \end{aligned} \quad (12)$$

The $L^\infty(\Omega)$ -norm [18, Chap. 9] of \mathcal{K}_j , $j = 1, 2$, is given by

$$\|\mathcal{K}_j\|_{L^\infty(\Omega)} = \operatorname{ess\,sup}_{t \in \Omega} \int_{\Omega} |\mathcal{K}_j(t, y; \zeta)| dy, \quad (13)$$

so that $\|\mathcal{K}_j\|_{L^\infty(\Omega)} \leq \kappa^2/2$ [2]. The resolvent \mathcal{R}_j of this operator exists and is given by the Neumann series $\mathcal{R}_j = \sum_{n=1}^{\infty} \mathcal{K}_n^{(j)}$ where $\mathcal{K}_n^{(j)} = \mathcal{K}_j \circ \mathcal{K}_{n-1}^{(j)}$ with $\mathcal{K}_1^{(j)} = \mathcal{K}_j$. It can also be shown using the methods in [2] that $\|\mathcal{K}_n^{(j)}\|_{L^\infty(\Omega)} \leq \kappa^{2n}/(2n)!$, yielding the estimate $\|\mathcal{R}_j\|_{L^\infty(\Omega)} \leq [\cosh(\kappa) - 1]$.

For $j = 2$, the solution of the Volterra integral equation can be stated as

$$\tilde{\mathbf{P}}_2(t; \zeta) = \Phi_2(t; \zeta) + \mathcal{R}_2[\Phi_2](t; \zeta). \quad (14)$$

From the estimate $\|\Phi_2(t; \zeta)\|_{L^\infty} \leq \kappa$ and

$$\begin{aligned} \|\mathcal{K}_1^{(2)}[\Phi_2](t; \zeta)\|_{L^\infty(\Omega)} &\leq \frac{\kappa^3}{2 \cdot 3}, \\ \|\mathcal{K}_2^{(2)}[\Phi_2](t; \zeta)\|_{L^\infty(\Omega)} &\leq \frac{\kappa^5}{2 \cdot 3 \cdot 4 \cdot 5}, \\ &\dots, \end{aligned}$$

we have $\|\tilde{\mathbf{P}}_2(t; \zeta)\|_{L^\infty} \leq \sinh \kappa$ for $\zeta \in \overline{\mathbb{C}}_+$. For $j = 1$, the solution of the Volterra integral equation can be stated as

$$\tilde{\mathbf{P}}_1(t; \zeta) = \Phi_1(t; \zeta) + \mathcal{R}_1[\Phi_1](t; \zeta). \quad (15)$$

From the estimate $\|\Phi_1(t; \zeta)\|_{L^\infty} \leq \kappa^2/2$ and

$$\begin{aligned} \|\mathcal{K}_1^{(1)}[\Phi_1](t; \zeta)\|_{L^\infty(\Omega)} &\leq \frac{\kappa^4}{2 \cdot 3 \cdot 4}, \\ \|\mathcal{K}_2^{(1)}[\Phi_1](t; \zeta)\|_{L^\infty(\Omega)} &\leq \frac{\kappa^6}{2 \cdot 3 \cdot 4 \cdot 5 \cdot 6}, \\ &\dots, \end{aligned}$$

we have $\|\tilde{\mathbf{P}}_1(t; \zeta)\|_{L^\infty} \leq [\cosh(\kappa) - 1]$ for $\zeta \in \overline{\mathbb{C}}_+$.

For the case $\zeta \in \mathbb{C}_-$, we consider $\tilde{\mathbf{P}}_-(t; \zeta) = \tilde{\mathbf{P}}(t; \zeta)e^{-2i\zeta t}$ so that $\tilde{\mathbf{P}}_-(T_+; \zeta) = ([a(\zeta) - 1]e^{-2i\zeta T_+}, b(\zeta))^\top$. The Volterra integral equations for $\tilde{\mathbf{P}}_-(t; \zeta) = (\tilde{\mathbf{P}}_1^{(-)}, \tilde{\mathbf{P}}_2^{(-)})^\top$ reads as:

$$\tilde{\mathbf{P}}_j^{(-)}(t; \zeta) = \Phi_j^{(-)}(t; \zeta) + \int_{\Omega} \mathcal{K}_j^{(-)}(t, y; \zeta) \tilde{\mathbf{P}}_j^{(-)}(y; \zeta) dy, \quad (16)$$

where $\Phi_j^{(-)}(t; \zeta) = \Phi_j(t; \zeta)e^{-2i\zeta t}$ and the Volterra kernels are given by

$$\begin{aligned} \mathcal{K}_1^{(-)}(x, y; \zeta) &= r(y) \int_y^x q(z) e^{-2i\zeta(x-z)} dz, \\ \mathcal{K}_2^{(-)}(x, y; \zeta) &= q(y) \int_y^x r(z) e^{-2i\zeta(z-y)} dz, \end{aligned} \quad (17)$$

with $\mathcal{K}_-(x, y; \zeta) = 0$ for $y > x$. Using the approach outlined above, it can be shown that, for $\zeta \in \mathbb{C}_-$, $\|\tilde{\mathbf{P}}_1^{(-)}(t; \zeta)\|_{L^\infty(\Omega)} \leq [\cosh(\kappa) - 1]e^{-2\operatorname{Im}(\zeta)T_-}$ and $\|\tilde{\mathbf{P}}_2^{(-)}(t; \zeta)\|_{L^\infty(\Omega)} \leq \sinh(\kappa)e^{-2\operatorname{Im}(\zeta)T_-}$.

Now combining the two cases, we obtain the results (9) and (10).

The result (11) follows from Lemma II.2. The proof of this lemma is provided in the Appendix A which is similar to that of the Riemann-Lebesgue lemma [19, Chap. 13]. \square

Lemma II.2. Let $q \in L^1$ be supported in Ω , then

$$\lim_{\xi \in \mathbb{R}, |\xi| \rightarrow \infty} \|\Phi_2(t; \xi + i\eta)\|_{L^\infty(\Omega)} = 0, \quad (18)$$

for fixed $\eta \in \mathbb{R}$ and $|\eta| < \infty$.

An immediate consequence of the preceding theorem together with the Paley-Wiener theorem [20, Chap. VI] is that

$$\operatorname{supp} \mathcal{F}^{-1}[f] \subset [-2T_+, 2T_-]. \quad (19)$$

The Fourier transformation in the above equation is understood in the sense of distributions.

Let us assume that $a(\zeta)$ has no zeros in $\overline{\mathbb{C}}_+$. Consider the limit $\lim_{r \rightarrow \infty} \log [1/|a(re^{i\theta})|] = 0$ for $0 \leq \theta \leq \pi$. Then there exists a constant $M > 0$ such that $|a(\zeta)|^{-1} \leq M$, for $\zeta \in \overline{\mathbb{C}}_+$. Therefore, $1/a(\zeta)$ is of exponential type zero in $\overline{\mathbb{C}}_+^1$. Then from Theorem II.1, it follows that $\rho(\zeta)$ is of exponential type $2T_+$ in $\overline{\mathbb{C}}_+$. In particular,

$$|\rho(\zeta)| \leq C M e^{2T_+ \operatorname{Im} \zeta}, \quad \zeta \in \overline{\mathbb{C}}_+. \quad (21)$$

Therefore, $\operatorname{supp} \mathcal{F}^{-1}[\rho] \subset [-2T_+, \infty)$. It is clear from the analysis above that the decay behavior of $\rho(\zeta)$ is largely dictated by the behavior of the scattering coefficient $b(\zeta)$.

¹ This can also be confirmed by the exact representation of $\log |a(\zeta)|$ which is guaranteed by [21, Thm 6.5.4] in the upper-half plane:

$$\log |a(\zeta)| = \frac{\eta}{\pi} \int_{-\infty}^{\infty} \frac{\log |a(\sigma)|}{(\sigma - \xi)^2 + \eta^2} d\sigma, \quad (20)$$

where $\zeta = \xi + i\eta$ with $\xi \in \mathbb{R}$ and $\eta > 0$.

Next, consider the situation when the discrete spectrum of a time-limited signal is not empty. Let us mention that the nature of the discrete spectrum for time-limited signals is discussed in [2]. To summarize these properties, let us observe that all the scattering coefficient, namely, $a(\zeta)$, $\bar{a}(\zeta)$, $b(\zeta)$ and $\bar{b}(\zeta)$ are entire functions of ζ with $\bar{a}(\zeta) = a^*(\zeta^*)$ and $\bar{b}(\zeta) = b^*(\zeta^*)$. It is also straightforward to conclude that the relationship

$$a(\zeta)a^*(\zeta^*) + b(\zeta)b^*(\zeta^*) = 1, \quad (22)$$

holds for all $\zeta \in \mathbb{C}$. For any eigenvalue ζ_k , this relationship takes the form $b(\zeta_k)b^*(\zeta_k^*) = 1$. Therefore, the norming constants are given by $b_k = b(\zeta_k) = 1/b^*(\zeta_k^*)$.

Proposition II.3. *Let (ζ_k, b_k) be the eigenvalue and the corresponding norming constant belonging to the discrete spectrum of a time-limited signal; then*

$$b_k = b(\zeta_k) = 1/b^*(\zeta_k^*). \quad (23)$$

In the following, the space of complex-valued functions of bounded variation over \mathbb{R} is denoted by BV and the variation of any function $f \in \text{BV}$ over $\Omega \subset \mathbb{R}$ is denoted by $\mathcal{V}[f; \Omega]$. If $q \in \text{BV}$, then $\partial_t q \in L^1$ exists almost everywhere such that $\|\partial_t q\|_{L^1} \leq \mathcal{V}[q; \Omega]$ [19, Chap. 16]. Let $q^{(1)}$ be equivalent to $\partial_t q$ so that $\|q^{(1)}\|_{L^1} = \|\partial_t q\|_{L^1}$.

Proposition II.4. *Let $q \in \text{BV}$ with support in $\Omega = [-T_-, T_+]$ such that it vanishes on $\partial\Omega$. Define $\kappa = \|q\|_{L^1}$ and $D = \frac{1}{2}\|q\|_{L^\infty} + \|q\|_{L^1} + \frac{1}{2}\|q^{(1)}\|_{L^1}$; then, the estimate*

$$|b(\zeta)| \leq \frac{D \cosh(\kappa)}{1 + |\zeta|} \times \begin{cases} e^{2T_+ \text{Im} \zeta}, & \zeta \in \bar{\mathbb{C}}_+, \\ e^{-2T_- \text{Im} \zeta}, & \zeta \in \mathbb{C}_-, \end{cases} \quad (24)$$

holds. Further, if $\beta(\tau) = \mathcal{F}^{-1}[b](\tau)$, then

$$\text{supp } \beta \subset [-2T_+, 2T_-], \quad (25)$$

and $\beta \in L^1 \cap L^2$.

Proof. The proof follows the same line of reasoning as in Theorem II.1. Addressing the case $\zeta \in \bar{\mathbb{C}}_+$, consider the second component in the Volterra integral equation (6):

$$\widetilde{P}_2(t; \zeta) = \Phi_2(t; \zeta) + \mathcal{K}_2[\Phi_2](t; \zeta). \quad (26)$$

Recall that $\widetilde{P}_2(t; \zeta) = b(t; \zeta)e^{2i\zeta t}$ from (5). In the proof of Theorem II.1, it was shown that the solution of (26) can be stated as

$$\widetilde{P}_2(t; \zeta) = \Phi_2(t; \zeta) + \mathcal{R}_2[\Phi_2](t; \zeta), \quad (27)$$

where \mathcal{R}_2 is the resolvent of the kernel \mathcal{K}_2 defined in (8). From the observation $\|\mathcal{R}_2\|_{L^\infty(\Omega)} \leq [\cosh(\kappa) - 1]$, we obtain the estimate

$$\|\widetilde{P}_2(t; \zeta)\|_{L^\infty(\Omega)} \leq \cosh(\kappa)\|\Phi_2(t; \zeta)\|_{L^\infty(\Omega)}. \quad (28)$$

Now, for fixed $\zeta \in \bar{\mathbb{C}}_+$, using the fact that $q \in \text{BV}(\Omega)$ and that it vanishes on $\partial\Omega$, it is straightforward to show, using integration by parts, that

$$\|\Phi_2(t; \zeta)\|_{L^\infty} \leq \frac{D}{(1 + |\zeta|)}. \quad (29)$$

Plugging this result in (28) yields the case $\zeta \in \bar{\mathbb{C}}_+$ in (24).

Again, using integration by parts, for fixed $\zeta \in \mathbb{C}_-$, it is also straightforward to show that

$$\|\Phi_2^{(-)}(t; \zeta)\|_{L^\infty(\Omega)} \leq \frac{D}{(1 + |\zeta|)} e^{-2T_- \text{Im} \zeta}. \quad (30)$$

From (16), an estimate of the form

$$\|b(t; \zeta)\|_{L^\infty(\Omega)} \leq \cosh(\kappa)\|\Phi_2^{(-)}(t; \zeta)\|_{L^\infty(\Omega)}, \quad (31)$$

can be obtained which then yields the case $\zeta \in \mathbb{C}_-$ in (24).

The estimate in (24) shows that $b(\zeta)$ is of exponential-type in \mathbb{C} and the Paley-Wiener theorem [20, Chap. VI] ensures that $\text{supp } \beta \subset [-2T_+, 2T_-]$. The last part of the result requires the part (a) of Lemma II.5. \square

For the sake of convenience, let us introduce the following class of functions:

Definition II.1. *A function $F(\zeta)$ is said to belong to the class $H_+(T)$ if it is analytic in $\bar{\mathbb{C}}_+$ and satisfies the following estimate*

$$|F(\zeta)| \leq \frac{C}{1 + |\zeta|} e^{2T \text{Im} \zeta}, \quad \zeta \in \bar{\mathbb{C}}_+,$$

for some constant $C > 0$. Similarly, a function $F(\zeta)$ is said to belong to the class $H_-(T)$ if it is analytic in $\bar{\mathbb{C}}_-$ and satisfies the following estimate

$$|F(\zeta)| \leq \frac{C}{1 + |\zeta|} e^{-2T \text{Im} \zeta}, \quad \zeta \in \bar{\mathbb{C}}_-,$$

for some constant $C > 0$.

Clearly, if $F(\zeta) \in H_+(T)$, then $F^*(\zeta^*) \in H_-(T)$. The inverse Fourier-Laplace Transform of such functions is studied in the following lemma which is proved in the Appendix B:

Lemma II.5. *Let $F \in H_+(T)$ and define $f(\tau) = \mathcal{F}^{-1}[F](\tau)$.*

- (a) *The function $f(\tau)$ is supported in $[-2T, \infty)$ and belongs to $L^1 \cap L^2$.*
- (b) *Define $G(\zeta) = i\zeta F(\zeta) - \mu e^{-2i\zeta T}$ where μ is such that $G(\zeta)e^{2i\zeta T} \rightarrow 0$ as $|\zeta| \rightarrow \infty$ in $\bar{\mathbb{C}}_+$ and $G \in H_+(T)$. Let $g(\tau) = \mathcal{F}^{-1}[G](\tau)$; then, $g(\tau)$ is supported in $[-2T, \infty)$ and belongs to $L^1 \cap L^2$. Furthermore, $f(\tau) = \mu + \int_{-2T}^{\tau} g(\tau') d\tau'$ so that it has a finite limit as $\tau \rightarrow -2T + 0$ and it is bounded on $[-2T, \infty)$.*

Strengthening the regularity conditions on the potential allows us to strengthen the regularity results for $\beta(\tau)$ as evident from the following theorem:

Theorem II.6. *Let m be a finite positive integer. Let $q \in \mathbf{C}_0^{m+1}(\Omega)$. Then the function $\beta(\tau) = \mathcal{F}^{-1}[b](\tau)$ is such that $\text{supp } \beta(\tau) \subset [-2T_+, 2T_-]$ and it is m -times differentiable in $(-2T_+, 2T_-)$. Furthermore, $\partial_\tau^k \beta(\tau) \rightarrow 0$ as $\tau \rightarrow 2T_- -$ and $\tau \rightarrow -2T_+ +$ for all $0 \leq k \leq m$.*

Proof. The proof can be obtained by a repeated application of the Prop. II.4 as follows: We consider the second component of the Volterra integral equations (6) and (16). Let $R_0(t) = r(t)$ and define a sequence of functions

$$R_{k+1}(t) = \partial_t R_k(t) - r(t) \int_{-T_-}^t q(y) R_k(y) dy. \quad (32)$$

It can be shown that $R_k(t)$ is bounded on Ω for $k \leq m$. Further, set $\bar{P}_{2,0}(t; \zeta) = \bar{P}_2(t; \zeta) = b(t; \zeta) e^{2i\zeta t}$ and introduce a sequence of functions $\bar{P}_{2,k}(t; \zeta)$ as

$$\bar{P}_{2,k+1}(t; \zeta) = i\zeta \bar{P}_{2,k}(t; \zeta) + \frac{1}{2} R_k(t) \quad (33)$$

where $k \leq m$. Using mathematical induction, it can be shown that each of the iterates satisfy the integral equations given by

$$\bar{P}_{2,k}(t; \zeta) = \Phi_{2,k}(t; \zeta) + \int_{\Omega} \mathcal{K}_2(t, y; \zeta) \bar{P}_{2,k}(y; \zeta) dy, \quad (34)$$

where $0 \leq k \leq m+1$ with

$$\Phi_{2,k}(t; \zeta) = \frac{1}{2} \int_{-T_-}^t R_k(y) e^{2i\zeta(t-y)} dy. \quad (35)$$

Following the approach used in Prop. II.4, it can be shown that $b_k(\zeta) = \bar{P}_{2,k}(T_+; \zeta) e^{-2i\zeta T_+}$ belongs to $H_+(T_+) \cup H_-(T_-)$. Define $\beta_k(\tau) = \mathcal{F}^{-1}[b_k](\tau)$, $k > 0$, then it is evident that its support falls in $[-2T_+, 2T_-]$ (Paley-Wiener theorem).

Also, note that each of the pairs $b_k(\zeta)$ and $b_{k+1}(\zeta)$ for $0 \leq k \leq m$ satisfy the conditions of the Lemma II.5 (with $F = b_k(\zeta)$ and $G = b_{k+1}(\zeta)$); therefore, $\partial_\tau \beta_k(\tau) = \beta_{k+1}(\tau)$ almost everywhere. This implies that $\beta(\tau)$ is m -times differentiable with $\partial_\tau^k \beta(\tau) = \beta_k(\tau)$ for $0 \leq k \leq m$.

The limit $\lim_{\tau \rightarrow -2T_+ + 0} \beta_k(\tau) = -(1/2)R_k(T_+) = 0$ follows from the fact that

$$\lim_{\zeta \in \mathbb{C}_+, \zeta \rightarrow \infty} i\zeta b_k(\zeta) = -\frac{1}{2} R_k(T_+). \quad (36)$$

Now consider $\bar{b}_k = b_k^*(\zeta^*)$ so that $\mathcal{F}^{-1}[\bar{b}](\tau) = \beta^*(-\tau)$. The limit $\lim_{\tau \rightarrow -2T_- + 0} \beta_k^*(-\tau) = (1/2)R_k^*(T_+) = 0$ follows from the fact that

$$\lim_{\zeta \in \mathbb{C}_+, \zeta \rightarrow \infty} i\zeta \bar{b}_k(\zeta) = \frac{1}{2} R_k^*(T_+). \quad (37)$$

Therefore, $\beta_k(2T_- - 0) = 0$. \square

Remark II.1. Putting $\bar{\Omega} = [-2T_+, 2T_-]$, the preceding theorem states that if $q \in \mathbf{C}_0^{m+1}(\Omega)$, then $\beta \in \mathbf{C}_0^m(\bar{\Omega})$. It also follows that for every non-negative integer $k \leq m$ there exists a $D_k > 0$ such that

$$|b(\zeta)| \leq \frac{D_k}{(1 + |\zeta|)^k} \times \begin{cases} e^{2T_+ \text{Im} \zeta}, & \zeta \in \bar{\mathbb{C}}_+, \\ e^{-2T_- \text{Im} \zeta}, & \zeta \in \mathbb{C}_-. \end{cases} \quad (38)$$

Again, assuming that $a(\zeta)$ has no zeros in $\bar{\mathbb{C}}_+$, there exists $M > 0$ such that

$$|\rho(\zeta)| \leq \frac{D_k M}{(1 + |\zeta|)^k} e^{2T_+ \text{Im} \zeta}, \quad \zeta \in \bar{\mathbb{C}}_+. \quad (39)$$

1. Example: Doubly-truncated one-soliton potential

This example is taken from [9]. Let $q(t)$ denote the one-soliton potential with the discrete spectrum (ζ_1, b_1) where $\zeta = \xi_1 + i\eta_1$ so that

$$q(t) = \frac{4\eta_1 \beta_0}{1 + |\beta_0|^2}, \quad (40)$$

where $\beta_0(t; \zeta_1, b_1) = -(1/b_1)e^{-2i\zeta_1 t}$. We make the potential compactly supported by truncating the part which lies outside $[-T_-, T_+]$. Let the doubly-truncated version of $q(t)$ be denoted by $q^{(\Gamma)}(t)$. Note that, unlike $q(t)$, the doubly-truncated potential $q^{(\Gamma)}(t)$ is not reflectionless.

Let $2T = T_+ + T_-$ and define $Z_+ = 1/\beta_0(T_+)$ and $Z_- = \beta_0(-T_-)$ so that $|Z_\pm| = |b_1|^{\pm 1} e^{-2\eta_1 T_\pm}$. The scattering coefficients can be shown to be given by

$$a^{(\Gamma)}(\zeta) = 1 + \frac{2i\eta_1 Z_+^* Z_-^*}{\Xi} \left[\frac{e^{4i\zeta T} - e^{4i\zeta_1^* T}}{\zeta - \zeta_1^*} - \frac{e^{4i\zeta T} - e^{4i\zeta_1 T}}{\zeta - \zeta_1} \right], \quad (41)$$

and

$$b^{(\Gamma)}(\zeta) = \frac{2i\eta_1 b_1 |Z_-|^2}{\Xi} \frac{(e^{-2i(\zeta - \zeta_1)T_+} - e^{-2i(\zeta - \zeta_1)T_-})}{\zeta - \zeta_1} + \frac{2i\eta_1 |Z_+|^2}{b_1^* \Xi} \frac{(e^{-2i(\zeta - \zeta_1^*)T_+} - e^{-2i(\zeta - \zeta_1^*)T_-})}{\zeta - \zeta_1^*}, \quad (42)$$

where $\Xi = (1 + |Z_+|^2)(1 + |Z_-|^2)$. Putting $2T_0 = T_+ - T_-$, we have

$$\beta^{(\Gamma)}(\tau) = \frac{2\eta_1}{\Xi} e^{-i\xi_1 \tau} \left[b_1 |Z_-|^2 e^{\eta_1 \tau} + \frac{|Z_+|^2}{b_1^*} e^{-\eta_1 \tau} \right] \Pi\left(\frac{\tau + 2T_0}{2T}\right), \quad (43)$$

where $\Pi(\tau)$ denotes the rectangle function defined as

$$\Pi(\tau) = \begin{cases} 1, & |\tau| \leq 1, \\ 0, & \text{otherwise.} \end{cases} \quad (44)$$

B. The direct transform: One-sided signals

Let $\Omega = (-\infty, T_+]$ in the following paragraphs unless stated otherwise. For $d > 0$, consider the class of complex-valued functions supported in Ω , denoted by $\mathbf{E}_d(\Omega)$, such that for $f \in \mathbf{E}_d(\Omega)$, there exists $C > 0$ such that the estimate $|f(t)| \leq C e^{-2d|t|}$ holds almost everywhere in Ω . Clearly, $\mathbf{E}_d(\Omega) \subset L^p(\Omega)$ for $1 \leq p \leq \infty$.

For $q \in \mathbf{E}_d(\Omega)$, the scattering coefficients, $a(\zeta)$ and $b(\zeta)$, are analytic in $\bar{\mathbb{C}}_+$, (in fact the region of analyticity turns out to be $\text{Im} \zeta > -d$) [2]. The results in Theorem II.1 can now be modified as follows:

Theorem II.7. Let $q \in \mathbf{E}_d(\Omega)$ with support in Ω and set $\kappa = \|q\|_{L^1(\Omega)}$. Then the estimates

$$|b(\zeta)| \leq \sinh(\kappa) e^{2T_+ \text{Im} \zeta}, \quad (45)$$

$$|\tilde{a}(\zeta)| \leq [\cosh(\kappa) - 1] e^{2T_+ \text{Im} \zeta}, \quad (46)$$

where $\tilde{a}(\zeta)$ denotes $[a(\zeta) - 1]e^{-2i\zeta T_+}$, hold for $\zeta \in \overline{\mathbb{C}}_+$. And, for fixed $0 \leq \eta < \infty$, we have

$$\lim_{\xi \in \mathbb{R}, |\xi| \rightarrow \infty} |f(\xi + i\eta)| = 0, \quad (47)$$

where $f(\zeta)$ denotes either $b(\zeta)$ or $\tilde{a}(\zeta)$.

An immediate consequence of the preceding theorem is that

$$\text{supp } \mathcal{F}^{-1}[f] \subset [-2T_+, \infty). \quad (48)$$

The Fourier transformation in the above equation is understood in the sense of distributions.

When $a(\zeta)$ has no zeros in $\overline{\mathbb{C}}_+$, it follows from the Theorem II.7 that $\rho(\zeta)$ is of exponential type $2T_+$ in $\overline{\mathbb{C}}_+$, i.e., there exists a constant $C > 0$ such that

$$|\rho(\zeta)| \leq C e^{2T_+ \text{Im} \zeta}, \quad \zeta \in \overline{\mathbb{C}}_+. \quad (49)$$

Therefore, $\text{supp } \mathcal{F}^{-1}[\rho] \subset [-2T_+, \infty)$ which is the same result one would obtain if the signal was time-limited. Further, the fact that $b(\zeta)$ is analytic in $\overline{\mathbb{C}}_+$ implies that, for any eigenvalue ζ_k , the corresponding norming constant is given by $b_k = b(\zeta_k)$ [2].

We conclude this section with a modification of the Prop. II.4 for the class of one-sided signals introduced above:

Proposition II.8. *Let $q \in E_d(\Omega) \cap \text{BV}(\Omega)$, and, define $\kappa = \|q\|_{L^1(\Omega)}$ and $D = \frac{1}{2}\|q\|_{L^\infty(\Omega)} + \|q\|_{L^1(\Omega)} + \frac{1}{2}\|q^{(1)}\|_{L^1(\Omega)}$. Then the estimate*

$$|b(\zeta)| \leq \frac{D \cosh(\kappa)}{1 + |\zeta|} e^{2T_+ \text{Im} \zeta}, \quad \zeta \in \overline{\mathbb{C}}_+, \quad (50)$$

holds. Further, if $\beta(\tau) = \mathcal{F}^{-1}[b](\tau)$, then

$$\text{supp } \beta \subset [-2T_+, \infty), \quad (51)$$

and $\beta \in L^1 \cap L^2$.

1. Example: Truncated one-soliton potential

This example has been previously treated in [9–13]. Consider the one-soliton potential discussed in Sec. II A 1. We make the potential one-sided by truncating the part which lies outside $(-\infty, T_+]$. Let the one-sided version of $q(t)$ be denoted by $q^{(-)}(t)$. Note that, unlike $q(t)$, the one-sided potential $q^{(-)}(t)$ is not reflectionless. Using the quantities defined in Sec. II A 1, the scattering coefficients work out to be

$$a^{(-)}(\zeta) = \frac{|Z_+|^2}{1 + |Z_+|^2} + \frac{1}{1 + |Z_+|^2} \left(\frac{\zeta - \zeta_1}{\zeta - \zeta_1^*} \right), \quad (52)$$

and

$$b^{(-)}(\zeta) = \frac{Z_+}{1 + |Z_+|^2} \left(\frac{2i\eta_1}{\zeta - \zeta_1^*} \right) e^{-2i\zeta T_+}. \quad (53)$$

Let $\theta(\tau)$ be the Heaviside step-function, then

$$\beta^{(-)}(\tau) = \frac{2\eta_1 Z_+}{1 + |Z_+|^2} e^{-i\zeta_1^*(\tau + 2T_+)} \theta(\tau + 2T_+). \quad (54)$$

C. The inverse problem

In this section, we would like to address the converse of some of the results obtained above. Define the nonlinear impulse response as

$$p(\tau) = \mathcal{F}^{-1}[\rho](\tau) = \frac{1}{2\pi} \int_{-\infty}^{\infty} \rho(\xi) e^{-i\xi\tau} d\xi. \quad (55)$$

In the following, we would like to examine the solution of the inverse scattering problem when $p(\tau) \in L^1 \cap L^2$ with support in $[-2T_+, \infty)$. We first give an important result due to Epstein which estimates the energy in the tail of the scattering potential defined by

$$\mathcal{E}_+(T) = \int_T^{\infty} |q(t)|^2 dt. \quad (56)$$

For a given $p(\tau) \in L^1 \cap L^2$, define

$$\mathcal{I}_m(T) = \left[\int_{2T}^{\infty} |p(-\tau)|^m d\tau \right]^{1/m}; \quad (57)$$

then, we have the following result:

Proposition II.9 (Epstein [22]). *For a given $p(\tau) \in L^1 \cap L^2$, if there exists a time T such that $\mathcal{I}_1(T) < 1$; then, the estimate*

$$\mathcal{E}_+(T) \leq \frac{2\mathcal{I}_2^2(T)}{[1 - \mathcal{I}_1^2(T)]},$$

holds provided $p(\tau)$ is continuous in the half-space $(-\infty, -2T)$.

Proof. Consider the Jost solutions with prescribed asymptotic behavior as $x \rightarrow \infty$:

$$\psi(t; \zeta) = \begin{pmatrix} 0 \\ 1 \end{pmatrix} e^{i\zeta t} + \int_t^{\infty} e^{i\zeta s} \mathbf{A}(t, s) ds, \quad (58)$$

where \mathbf{A} is independent of ζ . Consider the Gelfand-Levitan-Marchenko (GLM) integral equations. In the following we fix $t \in \mathbb{R}$ so that the GLM equations for $y \in \Omega_t = [t, \infty)$ is given by

$$\begin{aligned} A_2^*(t, y) &= - \int_t^{\infty} A_1(t, s) f(s + y) ds, \\ A_1^*(t, y) &= f(t + y) + \int_t^{\infty} A_2(t, s) f(s + y) ds, \end{aligned} \quad (59)$$

where $f(\tau) = p(-\tau)$. The solution of the GLM equations allows us to recover the scattering potential using $q(t) = -2A_1(t, t)$ together with the estimate $\|q\chi_{[t, \infty)}\|_2^2 = -2A_2(t, t)$ where χ_Ω denotes the characteristic function of $\Omega \subset \mathbb{R}$. Define the operator \mathcal{K} as

$$\begin{aligned} \mathcal{K}[g](y) &= \int_t^{\infty} ds \int_t^{\infty} dx f^*(y + s) f(s + x) g(x) \\ &= \int_t^{\infty} \mathcal{K}(y, x; t) g(x) dx, \end{aligned} \quad (60)$$

where the kernel function $\mathcal{K}(y, x; t)$ is given by

$$\mathcal{K}(y, x; t) = \int_t^\infty ds f^*(y+s)f(s+x). \quad (61)$$

The GLM equations in (59) can now be stated as

$$A_j(t, y) = \Phi_j(t, y) - \mathcal{K}[A_j(t, \cdot)](y), \quad j = 1, 2, \quad (62)$$

which is a Fredholm integral equation of the second kind where

$$\begin{aligned} \Phi_1(t, y) &= f^*(t+y), \\ \Phi_2(t, y) &= - \int_t^\infty f^*(y+s)f(t+s)ds. \end{aligned} \quad (63)$$

Recalling $\mathcal{I}_m(t) = \|f\chi_{[2t, \infty)}\|_{L^m}$ for $m = 1, 2, \infty$, we have

$$\begin{aligned} \|\mathcal{K}\|_{L^\infty(\Omega_t)} &= \text{ess sup}_{y \in \Omega_t} \int_t^\infty dx |\mathcal{K}(y, x; t)| \\ &\leq \text{ess sup}_{y \in \Omega_t} \int_t^\infty dx \int_t^\infty ds |f(y+s)||f(s+x)| \\ &\leq \text{ess sup}_{y \in \Omega_t} \int_{t+y}^\infty du |f(u)| \int_{t+u-y}^\infty du |f(u)| \\ &\leq [\mathcal{I}_1(t)]^2, \end{aligned} \quad (64)$$

and, $\|\Phi_2(t, \cdot)\|_{L^\infty(\Omega_t)} \leq [\mathcal{I}_2(t)]^2$. If $\mathcal{I}_1(t) < 1$, then the standard theory of Fredholm equations suggests that the resolvent of the operator \mathcal{K} exists [18]. Under this assumption, from (62), we have

$$\begin{aligned} \|A_j(t, \cdot)\|_{L^\infty(\Omega_t)} &\leq \|\Phi_j(t, \cdot)\|_{L^\infty(\Omega_t)} \\ &\quad + \|\mathcal{K}\|_{L^\infty(\Omega_t)} \|A_j(t, \cdot)\|_{L^\infty(\Omega_t)}, \end{aligned}$$

which yields

$$\begin{aligned} \|A_1(t, \cdot)\|_{L^\infty(\Omega_t)} &\leq \frac{\mathcal{I}_\infty(t)}{[1 - \mathcal{I}_1^2(t)]}, \\ \|A_2(t, \cdot)\|_{L^\infty(\Omega_t)} &\leq \frac{\mathcal{I}_2^2(t)}{[1 - \mathcal{I}_1^2(t)]}. \end{aligned} \quad (65)$$

Given that from here one can only assert that $|A_j(t, y)| \leq \|A_j(t, \cdot)\|_{L^\infty(\Omega_t)}$ almost everywhere (a.e.), we need to ascertain the continuity of $A_j(t, y)$ with respect to y throughout the domain Ω_t or as $y \rightarrow t$ from above. Assume that $f(\tau)$ is continuous, then $\Phi_j(t, y)$ is continuous with respect to y . It can be seen that the kernel function $\mathcal{K}(y, x; t)$ is also continuous with respect to y . Therefore, if the resolvent kernel is continuous (w.r.t. y) then the result follows. To this end, consider the Neumann series for the resolvent $\mathcal{R} = \sum_{n \in \mathbb{Z}_+} (-1)^n \mathcal{K}_n$ where $\mathcal{K}_n = \mathcal{K} \circ \mathcal{K}_{n-1}$ with $\mathcal{K}_1 = \mathcal{K}$. For fixed t , the partial sums $\sum_{1 \leq n \leq N} \|\mathcal{K}_n\|_{L^\infty(\Omega_t)} \leq [1 - \mathcal{I}_1^2(t)]^{-1}$ for all $N < \infty$. Therefore, uniform convergence of the partial sums allows us to conclude the continuity of the limit of the partial sums. \square

Corollary II.10. Consider $p(\tau) \in L^1 \cap L^2$ with support in $[-2T_+, \infty)$. If the solution of the GLM equation (59) exists, then

$$\text{supp } q \subset (-\infty, T_+]. \quad (66)$$

Proof. The proof is an immediate consequence of Prop. II.9 and the fact that $\mathcal{I}_j(t) = 0$, $j = 1, 2$ for all $t \in [T_+, \infty)$. \square

Remark II.2. The requirement that $p(\tau) \in L^1 \cap L^2$ in the corollary above can be weakened as long as the existence of the GLM equations can be guaranteed. Setting $f(\tau) = p(-\tau)$ and observing that $\text{supp } f \subset (-\infty, 2T_+]$, we may write the GLM equations as

$$\begin{aligned} A_2^*(t, y) &= - \int_t^{2T_+-y} A_1(t, s)f(s+y)ds, \\ A_1^*(t, y) &= f(t+y) + \int_t^{2T_+-y} A_2(t, s)f(s+y)ds. \end{aligned}$$

If the solution $A_j(t, y)$ exists, then $\text{supp}_y A_j(t, y) \subset [t, 2T_+ - t]$, $j = 1, 2$. Therefore, $A_j(t, y) \equiv 0$ for $t > T_+$ yielding $\text{supp } q \subset (-\infty, T_+]$.

Existence of the solution of the GLM equation (59) for a given $p(\tau) \in L^1 \cap L^2$ when $\mathcal{I}_1(T) > 1$ is established in [22]. The proof proceeds by observing that \mathcal{K} is a self-adjoint compact operator such that $\|\mathcal{K}\|_{L^2(\Omega_t)} \leq [\mathcal{I}_1(t)]^2$ which follows from

$$\begin{aligned} \|\mathcal{K}[g]\|_{L^2(\Omega_t)}^2 &= \int_t^\infty dy \left| \int_t^\infty dx \mathcal{K}(y, x; t)g(x) \right|^2 \\ &\leq \int_t^\infty dy \left[\int_t^\infty dx |\mathcal{K}(y, x; t)| \int_t^\infty dx |\mathcal{K}(y, x; t)| |g(x)|^2 \right] \\ &\leq [\mathcal{I}_1(t)]^4 \|g\|_{L^2(\Omega_t)}^2, \end{aligned}$$

For

$$\left(1 + [\mathcal{I}_1(t)]^2\right)^{-1} < \lambda_t < 2 \left(1 + [\mathcal{I}_1(t)]^2\right)^{-1},$$

define

$$\mathcal{T}[g] = \lambda_t \mathcal{K}[g] - (1 - \lambda_t)g, \quad (67)$$

so that the Fredholm equation in (62) can be written as

$$A_j(t, y) = \lambda_t \Phi_j(t, y) - \mathcal{T}[A_j(t, \cdot)](y), \quad j = 1, 2. \quad (68)$$

The resolvent of the operator \mathcal{T} exists as a consequence of the fact that $\|\mathcal{T}\|_2 < 1$. If $f(\tau)$ is continuous, the continuity of $A_j(t, y)$ for fixed t follows from the uniform convergence of the Neumann series.

We state the following result which specifies the sufficient conditions for the $\beta(\tau)$ for the scattering potential to be compactly supported:

Theorem II.11. Let $\beta(\tau) = \mathcal{F}^{-1}[b](\tau) \in \text{BV}$ with its support in $\tilde{\Omega} = [-2T_+, 2T_-]$ such that it vanishes on $\partial\tilde{\Omega}$. If $|b(\xi)| < 1$ for $\xi \in \mathbb{R}$, then, there exists a unique soliton-free scattering potential $q \in L^\infty$ such that

$$\text{supp } q \subset [-T_-, T_+].$$

Proof. The condition in the first part of the theorem guarantees that $p(\tau) \in L^1 \cap L^2$ is continuous with $\text{supp } p \subset [-2T_+, \infty)$. The proof for $\text{supp } q \subset (-\infty, T_+]$ follows from the preceding discussion. This also shows that $\text{supp } q^*(-t) \subset (-\infty, T_-]$ by considering $b^*(\xi)$ in place of $b(\xi)$. Combining the two cases allows us to conclude that $\text{supp } q \subset [-T_-, T_+]$.

Now, it remains to show that $q \in L^\infty$. Setting $f(\tau) = p(-\tau)$ and considering the support of $f(\tau)$, we may write the GLM equations as

$$\begin{aligned} A_2^*(t, y) &= - \int_t^{2T_+ - y} A_1(t, s) f(s + y) ds, \\ A_1^*(t, y) &= f(t + y) + \int_t^{2T_+ - y} A_2(t, s) f(s + y) ds. \end{aligned} \quad (69)$$

This allows us to conclude that $\text{supp}_y A_1(t, y) \subset [t, 2T_+ - t]$. Further, from the continuity of $A_1(t, y)$ with respect to y over the bounded set $[t, 2T_+ - t]$, it follows that $q(t) = -2A_1(t, t)$ is bounded. \square

Note that the discussion in the preceding paragraphs where the starting point of the discussion was $p(\tau)$ does not require explicit assumption about the presence/absence of the bound states. However, when starting with $\beta(\tau)$, this assumption is required in order to construct $p(\tau)$.

1. Presence of bound states

Let us start our discussion with one-sided signals supported in $\Omega = (-\infty, T_+]$. In this case, $b(\zeta)$ is analytic in $\overline{\mathbb{C}}_+$ and, for any eigenvalue ζ_k , the corresponding norming constant is given by $b_k = b(\zeta_k)$ [2]. Let us show that this condition is sufficient to guarantee the one-sided support of $q(t)$. To this end, we first prove the following lemma which specifies the support of $p(\tau)$:

Lemma II.12. *Let $b(\zeta) \in H_+(T_+)$ with $|b(\xi)| < 1$ for $\xi \in \mathbb{R}$. Let the discrete spectrum be given by $\mathfrak{S}_K = \{(\zeta_k, b_k)\}$, $b_k = b(\zeta_k)$, $k = 1, 2, \dots, K$, then*

$$\text{supp } p \subset [-2T_+, \infty). \quad (70)$$

Proof. For $\kappa > 0$, consider the contours $\Gamma_\kappa = \{\zeta \in \mathbb{R} \mid |\zeta| \leq \kappa\}$ and $C_\kappa = \{\zeta \in \overline{\mathbb{C}}_+ \mid |\zeta| = \kappa\}$. The radiative part of the reflection coefficient is given by $\rho_R(\zeta) = \rho(\zeta)a_S(\zeta)$ where $a_S(\zeta) = \prod_{k=1}^K (\zeta - \zeta_k)/(\zeta_k - \zeta_k^*)$. Then the condition on $b(\zeta)$ guarantees that $\rho_R \in H_+(2T_+)$. For sufficiently large κ , using Cauchy's theorem, we have

$$\mathcal{I}_\kappa(\tau) = \frac{1}{2\pi i} \oint_{\Gamma_\kappa \cup C_\kappa} \rho(\zeta) e^{i\zeta\tau} = \sum_k \text{Res}[\rho; \zeta_k] e^{i\zeta_k\tau}, \quad (71)$$

where the contour $\Gamma_\kappa \cup C_\kappa$ is oriented positively. For $\tau > 2T_+$, the integrand on C_κ is exponentially decaying with respect to κ . Therefore, in the limit $\kappa \rightarrow \infty$, for $\tau > 2T_+$,

$$f(\tau) = \frac{1}{2\pi} \int_{\mathbb{R}} \rho(\zeta) e^{i\zeta\tau} - i \sum_k \text{Res}[\rho; \zeta_k] e^{i\zeta_k\tau} = 0, \quad (72)$$

where we have used the fact that $\text{Res}[\rho; \zeta_k] = b(\zeta_k)/\dot{a}(\zeta_k)$. Now, the conclusion (70) follows from $p(\tau) = f(-\tau)$. \square

This lemma ensures that $\text{supp } q \subset (-\infty, 2T_+]$. However, given the exponentially increasing behavior of $p(\tau)$, one can only assert that $\|q\chi_{[t, T_+]}\|_2$ is finite for finite t . This question will be addressed later using a rather direct approach where such results can be obtained trivially.

Remark II.3. *Define $\sigma(\zeta) = b^*(\zeta^*)/a(\zeta)$. Proceeding as in Lemma II.12, it can also be concluded that if $b(\zeta) \in H_-(T_-)$ and $|b(\xi)| < 1$ then $1/b_k = b^*(\zeta_k^*)$ implies $s(\tau) = \mathcal{F}^{-1}[\sigma](\tau)$ is supported in $[-2T_-, \infty)$.*

The remark shows that $\text{supp } q^*(-t) \subset [-2T_-, \infty)$. Combining the two cases, it immediately follows that $\text{supp } q \subset [-T_-, T_+]$. Note that similar arguments can be found in [2, App. 5] where the authors have characterized the nature of the nonlinear Fourier spectrum corresponding to a time-limited signal. The difference merely lies in what is considered as the starting point. Starting from a one-sided $p(\tau)$ does not always lead to a compactly supported $\beta(\tau)$; therefore, it is much more convenient to start with an exponential type $b(\zeta)$ or compactly supported $\beta(\tau)$. However, this does not guarantee that $b(\zeta_k) = b_k$ and $b(\zeta_k^*) = 1/b_k^*$ are satisfied at the same time. It appears that without losing a certain degree of freedom in choosing $\beta(\tau)$, arbitrary bound states cannot be introduced in the scattering potential while maintaining its compact support.

Now let us discuss a direct approach which also provides some insight into the effective support of potential obtained as a result of addition of bound states to compactly supported (radiative) potentials. The Darboux transformation (DT) technique allows one to introduce bound states to any arbitrary potential referred to as the *seed* potential. In the following discussion, we assume that we have a compactly supported potential, $q_0(t)$, with its support in $[-T_-, T_+]$. For the sake of simplicity let us assume that the discrete spectrum of the seed potential is empty. The Jost solution of the seed potential, in matrix form, is denoted by $v_0 = (\phi_0, \psi_0)$. It is known that DT can be implemented as a recursive scheme [23] which is briefly summarized below. Let us define the successive discrete spectra $\emptyset = \mathfrak{S}_0 \subset \mathfrak{S}_1 \subset \mathfrak{S}_2 \subset \dots \subset \mathfrak{S}_K$ such that $\mathfrak{S}_j = \{(\zeta_j, b_j)\} \cup \mathfrak{S}_{j-1}$ for $j = 1, 2, \dots, K$ where (ζ_j, b_j) are distinct elements of \mathfrak{S}_K . The Darboux matrices of degree one can be stated as

$$D_1(t; \zeta, \mathfrak{S}_j | \mathfrak{S}_{j-1}) = \zeta \sigma_0 - \begin{pmatrix} |y_{j-1}|^2 \zeta_j + \zeta_j^* & (\zeta_j - \zeta_j^*) y_{j-1} \\ \frac{1 + |y_{j-1}|^2}{(\zeta_j - \zeta_j^*) y_{j-1}^*} & \frac{1 + |y_{j-1}|^2}{\zeta_j + \zeta_j^* |y_{j-1}|^2} \end{pmatrix}, \quad (73)$$

where

$$\gamma_{j-1}(t; \zeta_j, b_j) = \frac{\phi_1^{(j-1)}(t; \zeta_j) - b_j \psi_1^{(j-1)}(t; \zeta_j)}{\phi_2^{(j-1)}(t; \zeta_j) - b_j \psi_2^{(j-1)}(t; \zeta_j)}, \quad (74)$$

for $(\zeta_j, b_j) \in \mathfrak{S}_K$ and the successive Jost solutions, $v_j = (\phi_j, \psi_j)$, needed in this ratio are computed as

$$v_j(t; \zeta) = \frac{1}{(\zeta - \zeta_j^*)} D_1(t; \zeta, \mathfrak{S}_j | \mathfrak{S}_{j-1}) v_{j-1}(t; \zeta). \quad (75)$$

Let us denote the successive augmented potentials by $q_j(t)$ and

define

$$\begin{aligned}\mathcal{E}_j^{(-)}(t) &= \int_{-\infty}^t |q_j(s)|^2 ds, \\ \mathcal{E}_j^{(+)}(t) &= \int_t^{\infty} |q_j(s)|^2 ds.\end{aligned}\quad (76)$$

Then the potential is given by

$$q_j = q_{j-1} - 2i \frac{(\zeta_j - \zeta_j^*) \gamma_{j-1}}{1 + |\gamma_{j-1}|^2}, \quad (77)$$

and

$$\begin{aligned}\mathcal{E}_j^{(-)} &= \mathcal{E}_{j-1}^{(-)} + \frac{4 \operatorname{Im}(\zeta_j)}{1 + |\gamma_{j-1}|^2}, \\ \mathcal{E}_j^{(+)} &= \mathcal{E}_{j-1}^{(+)} + \frac{4 \operatorname{Im}(\zeta_j)}{1 + |\gamma_{j-1}|^2}.\end{aligned}\quad (78)$$

The above relations can be readily verified by computing the coefficient of ζ^0 and ζ^{-1} in the asymptotic expansion of $v_j(t, \zeta) e^{i\sigma_3 \zeta t}$ in the negative powers of ζ [2]. Now, if we were to truncate the augmented potential such that the support becomes $[-T'_-, T'_+]$ where $T_{\pm} \leq T'_{\pm}$, the energy in the tails can be computed exactly thanks to the recurrence relations for $\mathcal{E}_j^{(\pm)}$. Note that, for $T_- < t \leq -T'_-$, the seed Jost solution can be stated exactly:

$$\phi_0(t; \zeta) = \begin{pmatrix} 1 \\ 0 \end{pmatrix} e^{-i\zeta t}, \quad \psi_0(t; \zeta) = \begin{pmatrix} \bar{b}_0(\zeta) e^{-i\zeta t} \\ a_0(\zeta) e^{i\zeta t} \end{pmatrix}, \quad (79)$$

where $a_0(\zeta)$ and $b_0(\zeta)$ are the scattering coefficients of $q_0(t)$. Thus the energy content of the part of the signal supported in $(-\infty, -T'_-]$, denoted by $\mathcal{E}^{(-)}(-T'_-)$, using the recursive scheme stated above in (78). Now let us examine what happens when we assume $\bar{b}(\zeta_k) = 1/b_k$. For $k = 1$, we have $\gamma_1 = 0$ so that

$$v_1(t; \zeta) = \begin{pmatrix} 1 & 0 \\ 0 & \frac{\zeta - \zeta_1}{\zeta - \zeta_1^*} \end{pmatrix} v_0(t; \zeta),$$

so that

$$\phi_1(t; \zeta) = \begin{pmatrix} 1 \\ 0 \end{pmatrix} e^{-i\zeta t}, \quad \psi_1(t; \zeta) = \begin{pmatrix} \bar{b}_0(\zeta) e^{-i\zeta t} \\ a_1(\zeta) e^{i\zeta t} \end{pmatrix}, \quad (80)$$

where

$$a_1(\zeta) = \left(\frac{\zeta - \zeta_1}{\zeta - \zeta_1^*} \right) a_0(\zeta). \quad (81)$$

Using mathematical induction it can be shown that $\gamma_j = 0$ for $j = 0, 1, \dots, K$, and

$$\phi_j(t; \zeta) = \begin{pmatrix} 1 \\ 0 \end{pmatrix} e^{-i\zeta t}, \quad \psi_j(t; \zeta) = \begin{pmatrix} \bar{b}_0(\zeta) e^{-i\zeta t} \\ a_j(\zeta) e^{i\zeta t} \end{pmatrix}, \quad (82)$$

where

$$a_j(\zeta) = \left(\frac{\zeta - \zeta_j}{\zeta - \zeta_j^*} \right) a_{j-1}(\zeta). \quad (83)$$

Note that the arguments above are identical to those presented in [24] where $T'_{\pm} = \infty$. From here it is easy to conclude that $\mathcal{E}^{(-)}(-T'_-) \equiv 0$. For $t = T'_+$, similar arguments can be provided to conclude that, if $b(\zeta_k) = b_k$, the energy in the tail supported in $[T'_+, \infty)$, denoted by $\mathcal{E}^{(+)}(T'_+)$, is identically zero.

Let us conclude this section with the following observation: Even if the relations $b(\zeta_k) = b_k$ and $\bar{b}(\zeta_k) = 1/b_k$ are not satisfied, the augmented signal, $q_K(t)$, can still be considered as effectively supported within some $[-T'_-, T'_+]$ up to a tolerance, say ϵ , such that $\epsilon \|q_K\|_2^2 = \mathcal{E}^{(-)}(-T'_-) + \mathcal{E}^{(+)}(T'_+)$. Here, $\|q_K\|_2^2 = \mathcal{E}^{(-)}(T'_+) + \mathcal{E}^{(+)}(T'_+)$ with $\mathcal{E}_0^{(-)}(T'_+) = \|q_0\|_2^2$ which is assumed to be known.

III. NUMERICAL METHODS

Numerical methods for inverse scattering can be grouped into two classes: The first class of methods can be characterized as the *differential approach* which proceeds by discretizing the ZS problem using exponential one-step methods that admit of a layer-peeling property. The discrete framework thus obtained can be used for direct as well as inverse scattering². The second class of methods can be characterized as the *integral approach* which proceeds by discretizing the Gelfand-Levitan-Marchenko equations. The discrete framework thus obtained can be used for direct as well as inverse scattering with some limitations³.

A. Differential approach

In this section, we review the discretization scheme for the ZS problem first proposed in [14]. This scheme can be described as the exponential one-step method based on the trapezoidal rule of integration. In order to discuss the discretization scheme, we take an equispaced grid defined by $t_n = T_1 + nh$, $n = 0, 1, \dots, N$, with $t_N = T_2$ where h is the grid spacing. Define $\ell_-, \ell_+ \in \mathbb{R}$ such that $h\ell_- = T_-, h\ell_+ = T_+$. Further, let us define $z = e^{i\zeta h}$. For the potential functions sampled on the grid, we set $q_n = q(t_n)$, $r_n = r(t_n)$. Using the same convention, $U_n = U(t_n)$ and $\tilde{U}_n = \tilde{U}(t_n)$ where \tilde{U} is given by

$$\tilde{U} = e^{i\sigma_3 \zeta t} U e^{-i\sigma_3 \zeta t} = \begin{pmatrix} 0 & q e^{2i\zeta t} \\ r e^{-2i\zeta t} & 0 \end{pmatrix}. \quad (84)$$

² Note that not all exponential integrators admit of a layer-peeling property and their characterization remains an open problem. Besides, it's also not clear if the layer-peeling property is a necessary condition for such systems to admit of an inverse scattering algorithm.

³ The presence of bound states makes the nonlinear impulse response an increasing function of τ (the covariable of ξ) in a certain half-space making the GLM equations ill-conditioned for numerical computations. Therefore, the GLM based approach is used in this article only when the discrete spectrum is empty.

Define $\tilde{\phi} = (a(t; \zeta), b(t; \zeta))^\top$. By applying the trapezoidal rule to (4), we obtain

$$\tilde{\phi}_{n+1} = \left(\sigma_0 - \frac{h}{2} \tilde{U}_{n+1} \right)^{-1} \left(\sigma_0 + \frac{h}{2} \tilde{U}_n \right) \tilde{\phi}_n.$$

Setting $2Q_n = hq_n$, $2R_n = hr_n$ and $\Theta_n = 1 - Q_n R_n$ so that

$$\begin{aligned} \phi_{n+1} &= \frac{z^{-1}}{\Theta_{n+1}} \begin{pmatrix} 1 + z^2 Q_{n+1} R_n & z^2 Q_{n+1} + Q_n \\ R_{n+1} + z^2 R_n & R_{n+1} Q_n + z^2 \end{pmatrix} v_n \\ &= z^{-1} M_{n+1}(z^2) \phi_n, \end{aligned} \quad (85)$$

or, equivalently,

$$\begin{aligned} \phi_n &= \frac{z^{-1}}{\Theta_n} \begin{pmatrix} R_{n+1} Q_n + z^2 & -z^2 Q_{n+1} - Q_n \\ -R_{n+1} - z^2 R_n & 1 + z^2 Q_{n+1} R_n \end{pmatrix} \phi_{n+1} \\ &= z^{-1} \tilde{M}_{n+1}(z^2) \phi_{n+1}. \end{aligned} \quad (86)$$

In order to express the discrete approximation to the Jost solutions, let us define the vector-valued polynomial

$$P_n(z) = \begin{pmatrix} P_1^{(n)}(z) \\ P_2^{(n)}(z) \end{pmatrix} = \sum_{k=0}^n P_k^{(n)} z^k = \sum_{k=0}^n \begin{pmatrix} P_{1,k}^{(n)} \\ P_{2,k}^{(n)} \end{pmatrix} z^k. \quad (87)$$

The Jost solutions ϕ can be written in the form $\phi_n = z^\ell z^{-n} P_n(z^2)$. Note that this expression corresponds to the boundary condition $\phi_0 = z^\ell (1, 0)^\top$ which translate to $P_0 = (1, 0)^\top$. The other Jost solution, $\bar{\phi}_n$, can be written as $\bar{\phi}_n = z^{-\ell} z^n (i\sigma_2) P_n^*(1/z^{*2})$. The recurrence relation for the polynomial associated with the Jost solution takes the form

$$P_{n+1}(z^2) = M_{n+1}(z^2) P_n(z^2). \quad (88)$$

The discrete approximation to the scattering coefficients is obtained from the scattered field, $\phi_N = (a_N z^{-\ell_+}, b_N z^{\ell_+})^\top$, which yields

$$a_N(z^2) = P_1^{(N)}(z^2), \quad b_N(z^2) = (z^2)^{-\ell_+} P_2^{(N)}(z^2). \quad (89)$$

The quantities a_N and b_N above are referred to as the *discrete scattering coefficients*. Note that these coefficients can only be defined for $\text{Re } \zeta \in [-\pi/2h, \pi/2h]$.

1. The layer-peeling algorithm

Let us consider the problem of recovering the samples of the scattering potential from the discrete scattering coefficients known in the polynomial form. This step is referred to as the *discrete inverse scattering* step. Starting from the recurrence relation (88), the *layer-peeling* step consists in using $P_{n+1}(z^2)$ to retrieve the samples of the potential needed to compute the transfer matrix $\tilde{M}_{n+1}(z^2)$ so that the entire step can be repeated with $P_n(z^2)$ until all the samples of the potential are recovered.

Let us assume $Q_0 = 0$. The recurrence relation for the trapezoidal rule yields

$$P_{1,0}^{(n+1)} = \Theta_{n+1}^{-1} \prod_{k=1}^n \left(\frac{1 + Q_k R_k}{1 - Q_k R_k} \right) = \Theta_{n+1}^{-1} \prod_{k=1}^n \left(\frac{2 - \Theta_k}{\Theta_k} \right) \quad (90)$$

and $P_{n+1}^{(n+1)} = 0$. The last relationship follows from the assumption $Q_0 = 0$. For sufficiently small h , it is reasonable to assume that $1 + Q_n R_n = 2 - \Theta_n > 0$ so that $P_{1,0}^{(n)} > 0$ (it also implies that $|Q_n| = |R_n| < 1$). Now for the layer-peeling step, we have the following relations $R_{n+1} = P_{2,0}^{(n+1)} / P_{1,0}^{(n+1)}$ and

$$R_n = \frac{\chi}{1 + \sqrt{1 + |\chi|^2}}, \quad \chi = \frac{P_{2,1}^{(n+1)} - R_{n+1} P_{1,1}^{(n+1)}}{P_{1,0}^{(n+1)} - Q_{n+1} P_{2,0}^{(n+1)}}. \quad (91)$$

Note that $P_{1,0}^{(n+1)} \neq 0$ and $P_{1,0}^{(n+1)} - Q_{n+1} P_{2,0}^{(n+1)} \neq 0$. As evident from (85), the transfer matrix, $M_{n+1}(z^2)$, connecting $P_n(z^2)$ and P_{n+1} is completely determined by the samples R_{n+1} and R_n (with $Q_{n+1} = -R_{n+1}^*$ and $Q_n = -R_n^*$).

2. Discrete inverse scattering with the reflection coefficient

Let us assume that the reflection coefficient $\rho \in H_+(T_+)$ and define $\check{\rho}(\zeta) = \rho(\zeta) e^{2i\zeta T_+}$. In order to obtain the discrete scattering coefficients, we follow a method due to Lubich [25, 26] which is used in computing quadrature weights for convolution integrals. Introduce the function $\delta(z)$ as in [25, 26] which corresponds to the trapezoidal rule of integration: $\delta(z) = 2(1-z)/(1+z)$. Next, we introduce the coefficients $\check{\rho}_k$ such that

$$\check{\rho}\left(\frac{i\delta(z^2)}{2h}\right) = \sum_{k=0}^{\infty} \check{\rho}_k z^{2k}, \quad (92)$$

then using the Cauchy integral, we have the relation

$$\check{\rho}_k = \frac{1}{2\pi i} \oint_{|z|^2=q} \left[\check{\rho}\left(\frac{i\delta(z^2)}{2h}\right) \right] z^{-2k-2} d(z^2), \quad (93)$$

which can be easily computed using FFT. The input to the layer-peeling algorithm can then be taken to be

$$P_1^{(N)}(z^2) = 1, \quad P_2^{(N)}(z^2) = \left\{ \check{\rho}\left(\frac{i\delta(z^2)}{2h}\right) \right\}_N,$$

where the notation $\{\cdot\}_N$ implies truncation after N terms.

If $\rho(\zeta)$ decays sufficiently fast, then an alternative approach can be devised. Define the function $\check{\rho}(\tau)$ as

$$\check{\rho}(\tau) = \frac{1}{2\pi} \int_{-\infty}^{\infty} \check{\rho}(\xi) e^{-i\xi\tau} d\xi. \quad (94)$$

Note that for $\tau < 0$, the contour can be closed in the upper half-plane and the integrals would evaluate to zero; therefore, $\check{\rho}(\tau)$ is causal. If, in addition, $\check{\rho}(\zeta)$ is analytic in the strip $-\kappa \geq \text{Im } \zeta < 0$, the nonlinear impulse response $\check{\rho}(\tau)$ can be shown to decay exponentially away from the origin. A polynomial approximation for $\check{\rho}(\zeta)$ can be furnished by using the trapezoidal sum to approximate the integral

$$\check{\rho}(\zeta) = \int_0^{\infty} \check{\rho}(\tau) e^{i\zeta\tau} d\tau. \quad (95)$$

Let the grid spacing in the τ -domain be $2h$, then

$$\begin{aligned}\check{\rho}(\zeta) &\approx h\check{\rho}(0) + 2h \sum_{k=1}^{N-1} \check{\rho}(2hk) [e^{2i\zeta h}]^k \\ &= h\check{\rho}(0) + 2h \sum_{k=1}^{N-1} \check{\rho}(2hk) z^{2k}.\end{aligned}\quad (96)$$

Note that the endpoint $\tau_N = 2Nh$ is omitted because $\check{\rho}(\tau_N)$ is assumed to be vanishingly small. For fixed $\zeta \in \overline{\mathbb{C}}_+$, the approximation is $O(h^2)$ assuming that the error due to truncation at τ_N is negligible at least for $N > N_0$ where N_0 depends on the decay properties of $\check{\rho}(\tau)$ and h . The approximation above asserts that $\check{\rho}(\xi)$ is effectively supported in $[0, \pi/h]$. Note that the method discussed in [15] makes the assumption that $\rho(\xi)$ has a compact support which is independent of h .

If the integral for $\check{\rho}(\tau)$ cannot be evaluated exactly, we use the FFT algorithm to compute the integral. The decay property of $\check{\rho}(\xi)$, $\xi \in \mathbb{R}$, decides the convergence of the discrete Fourier sum used in FFT so that it may be necessary to employ large number of samples in order to get accurate results.

B. Integral approach

Let us assume that the reflection coefficient $\rho \in \mathbf{H}_+(T_+)$ and define $\check{\rho}(\zeta) = \rho(\zeta)e^{2i\zeta T_+}$ as in Sec. III A 2. Introducing

$$\begin{aligned}\mathcal{A}_1(t, y) &= A_1(T_+ - t, T_+ - y + t), \\ \mathcal{A}_2(t, y) &= A_2(T_+ - t, T_+ - t + y),\end{aligned}\quad (97)$$

the GLM equations can be put into the following form

$$\begin{aligned}\mathcal{A}_2^*(t, 2t - y) + \int_0^y \mathcal{A}_1(t, 2t - s) \check{\rho}(y - s) ds &= 0, \\ -\mathcal{A}_1^*(t, y) + \int_0^y \mathcal{A}_2(t, s) \check{\rho}(y - s) ds &= -\check{\rho}(y),\end{aligned}\quad (98)$$

for $0 \leq y \leq 2t \leq 2T = T_- + T_+$ where $\check{\rho}(\tau)$ is defined by (94). The scattering potential is recovered using

$$\begin{aligned}q(T_+ - t) &= -2A_1(T_+ - t, T_+ - t) \\ &= -2\mathcal{A}_1(t, 2t),\end{aligned}\quad (99)$$

with the L^2 -norm of the potential truncated to $(T_+ - t, T_+]$ is given by

$$\begin{aligned}\int_0^t |q(T_+ - s)|^2 ds &= -2A_2(T_+ - t, T_+ - t) \\ &= -2\mathcal{A}_2(t, 0).\end{aligned}\quad (100)$$

Defining the grid $y_{j+1} = y_j + 2h$ and setting $\check{\rho}_k = \check{\rho}(2kh)$, we have

$$\begin{aligned}\mathcal{A}_2^*(t, 2t - y_l) + 2h \sum_{j=0}^l \check{\rho}_{l-j} \mathcal{A}_1(t, 2t - y_j) - h\check{\rho}_0 \mathcal{A}_1(t, 2t - y_l) \\ - h\check{\rho}_l \mathcal{A}_1(t, 2t) = 0, \\ \mathcal{A}_1^*(t, y_k) - 2h \sum_{j=0}^k \check{\rho}_{k-j} \mathcal{A}_2(t, y_j) + h\check{\rho}_0 \mathcal{A}_2(t, y_k) \\ + h\check{\rho}_k \mathcal{A}_2(t, 0) = \check{\rho}_k.\end{aligned}$$

Setting $t_j = jh$ for $j = 0, \dots, N$ with $k, l \leq m$ and introducing the quadrature weights $\omega_k = 2h\check{\rho}_k$, $k > 0$ with $\omega_0 = h\check{\rho}_0$, we have

$$\begin{aligned}\mathcal{A}_2(t_m, y_l) + \sum_{j=l}^m \omega_{l-j}^\dagger \mathcal{A}_1^*(t_m, y_j) - \frac{1}{2} \omega_l^\dagger \mathcal{A}_1^*(t_m, y_m) = 0, \\ -\mathcal{A}_1^*(t_m, y_k) + \sum_{j=0}^k \omega_{k-j} \mathcal{A}_2(t_m, y_j) - \frac{1}{2} \omega_k \mathcal{A}_2(t_m, 0) = -\check{\rho}_k,\end{aligned}$$

where $\omega_{l-j}^\dagger = \omega_{j-l}^*$. Now, define the lower triangular Töplitz matrix $\Gamma^{(m)} = (\gamma_{jk}^{(m)})_{(m+1) \times (m+1)}$ where

$$\gamma_{jk}^{(m)} = \begin{cases} \omega_{j-k}, & j - k \geq 0, \\ 0, & \text{otherwise,} \end{cases} \quad j, k = 0, 1, \dots, m,$$

and the Töplitz matrix $G^{(m)}$ as

$$G^{(m)} = \begin{pmatrix} I^{(m)} & -\Gamma^{(m)\dagger} \\ \Gamma^{(m)} & I^{(m)} \end{pmatrix},$$

where $I^{(m)}$ is the $(m+1) \times (m+1)$ identity matrix and ‘ \dagger ’ denotes Hermitian conjugate. Next, we define the vectors

$$\mathcal{A}_j^{(m)} = (\mathcal{A}_j(t_m, 0), \mathcal{A}_j(t_m, y_1), \dots, \mathcal{A}_j(t_m, y_m))^\top, \quad j = 1, 2,$$

and put

$$\chi^{(m)} = \begin{pmatrix} \mathcal{A}_2^{(m)} \\ -\mathcal{A}_1^{(m)*} \end{pmatrix}; \quad (101)$$

then the linear system corresponding to the GLM equation reads as

$$G^{(m)} \chi^{(m)} = \begin{pmatrix} -h\chi_{2m+1}^{(m)} \check{\rho}^{(m)\ddagger} \\ -\check{\rho}^{(m)} + h\chi_0^{(m)} \check{\rho}^{(m)} \end{pmatrix}, \quad (102)$$

where $\omega^{(m)\ddagger}$ is the reverse numerated and conjugated form of $\omega^{(m)}$. The double-dagger operation (\ddagger) will be used to mean reversal of index numeration and complex conjugation in the rest of this article unless otherwise stated. In order to develop a fast method of solution of the linear system, Belai *et al.* [16] exploited the Töplitz structure of the matrix $G^{(m)}$. It is known that the inverse of a Töplitz matrix is a *persymmetric* matrix. Our aim is to determine $\chi_0^{(m+1)}$ and $\chi_{2m+3}^{(m+1)}$, the first and the last component of the vector $\chi^{(m+1)}$, respectively. Therefore, we focus on the first and the last column of the matrix $[G^{(m)}]^{-1}$ which must be of the form

$$\begin{pmatrix} \mathbf{u}^{(m)} \\ \mathbf{v}^{(m)} \end{pmatrix}, \quad \begin{pmatrix} -\mathbf{v}^{(m)\ddagger} \\ \mathbf{u}^{(m)\ddagger} \end{pmatrix}. \quad (103)$$

The complex conjugate of the first and the last row of $[G^{(m)}]^{-1}$ have the form

$$\begin{pmatrix} \mathbf{u}^{(m)} \\ -\mathbf{v}^{(m)} \end{pmatrix}^\top, \quad \begin{pmatrix} \mathbf{v}^{(m)\ddagger} \\ \mathbf{u}^{(m)\ddagger} \end{pmatrix}^\top. \quad (104)$$

Therefore, it follows that

$$G^{(m)} \begin{pmatrix} \mathbf{u}^{(m)} \\ \mathbf{v}^{(m)} \end{pmatrix} = \begin{pmatrix} 1 \\ 0 \\ \vdots \\ 0 \end{pmatrix}, \quad G^{(m)} \begin{pmatrix} -\mathbf{v}^{(m)\ddagger} \\ \mathbf{u}^{(m)\ddagger} \end{pmatrix} = \begin{pmatrix} 0 \\ \vdots \\ 0 \\ 1 \end{pmatrix}. \quad (105)$$

These relations translate to

$$\begin{aligned} u_0^{(m)} - \omega^{(m)*} \cdot \mathbf{v}^{(m)} &= 1, \\ \omega^{(m)\ddagger} \cdot \mathbf{u}^{(m)*} + v_m^{(m)*} &= 0, \end{aligned} \quad (106)$$

where ‘ \cdot ’ denotes the scalar product of two vectors. The *inner bordering* scheme can now be stated as follows:

- For $m = 0$, set

$$\begin{pmatrix} \mathbf{u}^{(0)} \\ \mathbf{v}^{(0)} \end{pmatrix} = \frac{1}{(1 + |\omega_0|^2)} \begin{pmatrix} 1 \\ -\omega_0 \end{pmatrix}. \quad (107)$$

- Introduce c_m and d_m , such that

$$\begin{aligned} \mathbf{u}^{(m+1)} &= c_m \begin{pmatrix} \mathbf{u}^{(m)} \\ 0 \end{pmatrix} + d_m^* \begin{pmatrix} 0 \\ -\mathbf{v}^{(m)\ddagger} \end{pmatrix}, \\ \mathbf{v}^{(m+1)} &= c_m \begin{pmatrix} \mathbf{v}^{(m)} \\ 0 \end{pmatrix} + d_m^* \begin{pmatrix} 0 \\ \mathbf{u}^{(m)\ddagger} \end{pmatrix}, \end{aligned} \quad (108)$$

where c_m and d_m are determined such that (105) holds for $m+1$. This yields $c_m = (1 + |\beta_m|^2)^{-1}$ and $d_m = -\beta_m c_m$ where

$$\begin{aligned} \beta_m &= \sum_{j=0}^m \omega_{m+1-j}^* u_j^{(m)*} \\ &= \omega^{(m+1)*} \cdot \begin{pmatrix} 0 \\ \mathbf{u}^{(m)\ddagger} \end{pmatrix} = \omega^{(m+1)\ddagger} \cdot \begin{pmatrix} \mathbf{u}^{(m)*} \\ 0 \end{pmatrix}. \end{aligned} \quad (109)$$

The recurrence relation for $u_0^{(m)}$ and $v_0^{(m)}$ can be solved explicitly: From $u_0^{(m+1)} = c_m u_0^{(m)}$, we have

$$u_0^{(m+1)} = c_m c_{m-1} \dots c_0; \quad (110)$$

and from $v_0^{(m+1)} = c_m v_0^{(m)}$, we have

$$\begin{aligned} v_0^{(m+1)} &= -c_m c_{m-1} \dots c_0 \frac{\omega_0}{1 + |\omega_0|^2} \\ &= -\frac{\omega_0}{1 + |\omega_0|^2} u_0^{(m+1)}. \end{aligned} \quad (111)$$

Now, in order to determine the components $\chi_0^{(m+1)}$ and $\chi_{2m+3}^{(m+1)}$, based on the discussion above, it is straightforward to setup the following system of equations

$$\begin{aligned} \chi_0^{(m+1)} &= \begin{pmatrix} \mathbf{u}^{(m+1)} \\ -\mathbf{v}^{(m+1)} \end{pmatrix}^* \cdot \begin{pmatrix} -h\chi_{2m+3}^{(m+1)} \check{\mathbf{p}}^{(m+1)\ddagger} \\ -\check{\mathbf{p}}^{(m+1)} + h\chi_0^{(m+1)} \check{\mathbf{p}}^{(m+1)} \end{pmatrix}, \\ \chi_{2m+3}^{(m+1)} &= \begin{pmatrix} \mathbf{v}^{(m+1)\ddagger} \\ \mathbf{u}^{(m+1)\ddagger} \end{pmatrix}^* \cdot \begin{pmatrix} -h\chi_{2m+3}^{(m+1)} \check{\mathbf{p}}^{(m+1)\ddagger} \\ -\check{\mathbf{p}}^{(m+1)} + h\chi_0^{(m+1)} \check{\mathbf{p}}^{(m+1)} \end{pmatrix}. \end{aligned} \quad (112)$$

In order to simplify this linear system above, we compute the scalar products using the relations (106) and (108) as follows:

$$\begin{aligned} 2h\mathbf{u}^{(m+1)*} \cdot \check{\mathbf{p}}^{(m+1)\ddagger} &= c_m \beta_m - 2hd_m \mathbf{v}^{(m)} \cdot \check{\mathbf{p}}^{(m)*} \\ &= c_m \beta_m + d_m (1 - u_0^{(m)} - \omega_0^* v_0^{(m)}) \\ &= \frac{c_m u_0^{(m)}}{1 + |\omega_0|^2} \beta_m. \end{aligned} \quad (113)$$

Set $\lambda_m \equiv u_0^{(m)} / (1 + |\omega_0|^2) \in \mathbb{R}_+$. Next, we have

$$\begin{aligned} 2h\mathbf{v}^{(m+1)} \cdot \check{\mathbf{p}}^{(m+1)*} &= 2hc_m \mathbf{v}^{(m)} \cdot \check{\mathbf{p}}^{(m)*} + d_m^* \beta_m, \\ &= \frac{c_m u_0^{(m)}}{1 + |\omega_0|^2} - 1 = \lambda_{m+1} - 1. \end{aligned} \quad (114)$$

Using these results, the linear system (112) can be stated as

$$\begin{aligned} (1 + \lambda_{m+1})\chi_0^{(m+1)} + \beta_m \lambda_{m+1} \chi_{2m+3}^{(m+1)} &= -\frac{1}{h} (1 - \lambda_{m+1}), \\ \beta_m^* \lambda_{m+1} \chi_0^{(m+1)} - (1 + \lambda_{m+1})\chi_{2m+3}^{(m+1)} &= \frac{1}{h} \lambda_{m+1} \beta_m^*. \end{aligned} \quad (115)$$

Note that if $\check{\rho}(\zeta)$ decays at least as $O(\zeta^{-2})$, then $\check{\rho}_0 = 0$ and $\omega_0 = 0$. Solving for the general case, we have

$$\int_0^{t_{m+1}} |q(T_+ - s)|^2 ds \approx -2\chi_0^{(m+1)} = \frac{2}{h\Delta_m} (1 - c_m \lambda_m^2), \quad (116)$$

and

$$q(T_+ - t_{m+1}) \approx 2\chi_{2m+3}^{(m+1)*} = -\frac{4\beta_m c_m \lambda_m}{h\Delta_m}, \quad (117)$$

where

$$\begin{aligned} \Delta_m &= [1 + 2c_m \lambda_m + c_m \lambda_m^2] \\ &= [1 + 2c_m u_0^{(m)} + c_m (u_0^{(m)})^2] + O(h^2). \end{aligned} \quad (118)$$

The algorithm proposed by Belai *et al.* [16, 17] uses the approximations $c_m \approx 1$ and $u_0^{(m)} \approx 1$ in (117) while maintaining the accuracy of $O(h^2)$; however, this step may lead to higher truncation error on account of the relation (110) since

$$u_0^{(m)} = 1 - \sum_{k=0}^{m-1} |\beta_m|^2 + \dots \quad (119)$$

C. Discrete inverse scattering with the b-coefficient

Let the b -coefficient be of exponential-type such that its Fourier-Laplace transform, $\beta(\tau)$, is supported in $[-2T_+, 2T_-]$. Let $\check{b}(\zeta) = b(\zeta)e^{2i\zeta T_+}$ so that

$$\check{b}(\zeta) = \int_0^{2W} \check{\beta}(\tau) e^{i\zeta\tau} d\tau, \quad (120)$$

where $W = T_+ + T_-$ and $\check{\beta}(\tau)$ is the shifted version of $\beta(\tau)$ with support in $[0, 2W]$. We assume that $\check{\beta}(\tau)$ has derivatives

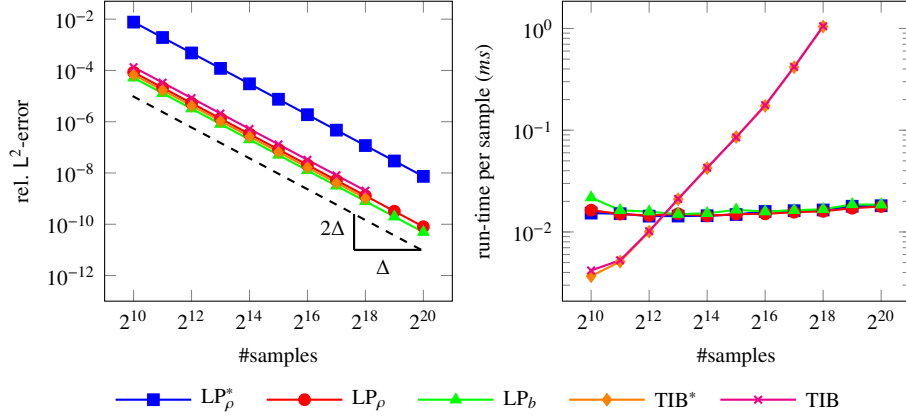


FIG. 1. The figure shows a comparison of the algorithms LP_ρ^* , LP_ρ , LP_b , TIB^* and TIB for the secant-hyperbolic potential ($A_R = 0.4$) with respect to convergence rate (left) and run-time per sample (right).

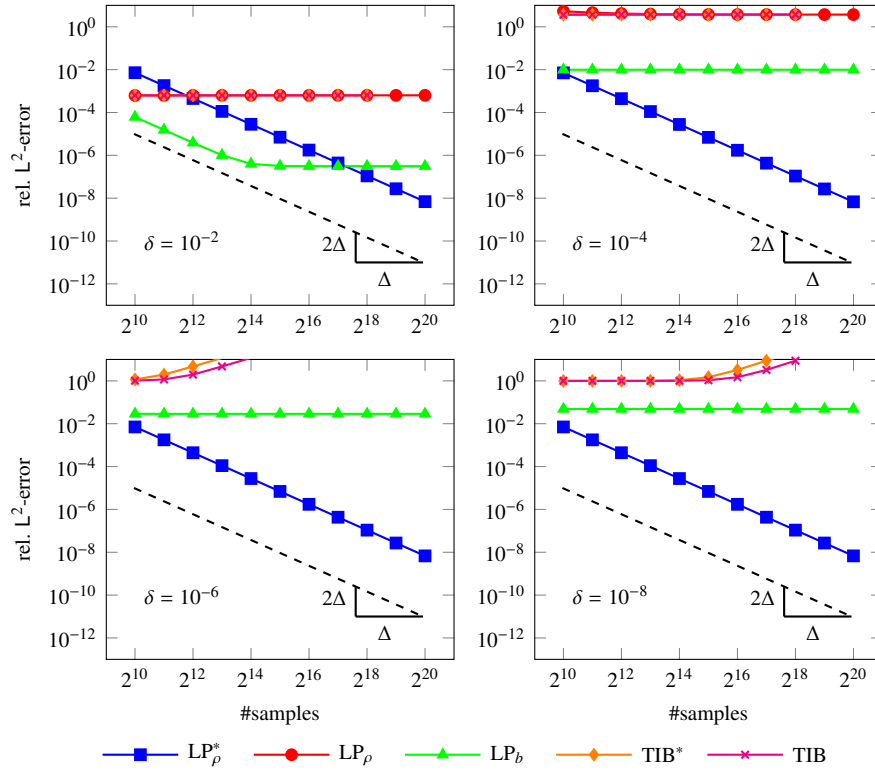


FIG. 2. The figure shows the convergence behavior of the algorithms LP_ρ^* , LP_ρ , LP_b , TIB^* and TIB for the secant-hyperbolic potential with $A_R = 0.5 - \delta$.

of order > 2 in $(0, 2W)$ and they vanish at the end points so that the integral can be approximated by the sum

$$\check{b}(\zeta) \approx 2h \sum_{k=0}^{N-1} \check{\beta}(2hk) [e^{2i\zeta h}]^k = 2h \sum_{k=0}^{N-1} \check{\beta}(2hk) z^{2k}. \quad (121)$$

If $\check{\beta}(\tau)$ is smooth, then the approximation above achieves spectral accuracy otherwise it is at least $O(h^2)$ accurate. Again, if $\check{\beta}(\tau)$ cannot be evaluated exactly, we use the FFT algorithm to

compute the integral

$$\check{\beta}(\tau) = \frac{1}{2\pi} \int_{-\infty}^{\infty} \check{b}(\xi) e^{-i\xi\tau} d\xi. \quad (122)$$

The decay property of $\check{b}(\xi)$, $\xi \in \mathbb{R}$, decides the convergence of the discrete Fourier sum used in FFT so that it may be necessary to employ large number of samples in order to get accurate results.

The next step consists of constructing a polynomial approximation for $a(\zeta)$ in $|z| < 1$ (under the assumption that no bound

states are present). With a slight abuse of notation, let us denote the polynomial approximation for $\check{b}(\zeta)$ by $\check{b}_N(z^2)$ or simply $\check{b}(z^2)$ ⁴. Here, the relation [2, 3] $|a(\xi)|^2 + |\check{b}(\xi)|^2 = 1$, $\xi \in \mathbb{R}$, allows us to set up a Riemann-Hilbert (RH) problem for a sectionally analytic function

$$\tilde{g}(z^2) = \begin{cases} g(z^2) & |z| < 1, \\ -g^*(1/z^{*2}) & |z| > 1, \end{cases} \quad (123)$$

such that the jump condition is given by

$$\tilde{g}^{(-)}(z^2) - \tilde{g}^{(+)}(z^2) = \log[1 - |\check{b}(z^2)|^2], \quad |z| = 1, \quad (124)$$

where $\tilde{g}^{(-)}(z^2)$ and $\tilde{g}^{(+)}(z^2)$ denotes the boundary values when approaching the unit circle from $|z| < 1$ and $|z| > 1$, respectively. Note that for the jump function to be well-defined, we must have $|\check{b}(z^2)| < 1$. Let the jump function on the right hand side of (124) be denoted by $f(z^2)$ which can be expanded as a Fourier series

$$f(z^2) = \sum_{k \in \mathbb{Z}} f_k z^{2k}, \quad |z| = 1. \quad (125)$$

Now, the solution to the RH problem can be stated using the Cauchy integral [27, Chap. 14]

$$\tilde{g}(z^2) = \frac{1}{2\pi i} \oint_{|w|=1} \frac{f(w)}{z^2 - w} dw. \quad (126)$$

The function $g(z^2)$ analytic in $|z| < 1$ then works out to be

$$g(z^2) = \sum_{k \in \mathbb{Z}_+ \cup \{0\}} f_k z^{2k}, \quad |z| < 1. \quad (127)$$

Finally, $a_N(z^2) = \{\exp[g(z^2)]\}_N$ with $z = e^{i\zeta h}$ where $\{\cdot\}_N$ denotes truncation after N terms. The implementation of the procedure laid out above can be carried out using the FFT algorithm, which involves computation of the coefficients f_k and the exponentiation in the last step. Note that, in the computation of $g(z^2)$, we discarded half of the coefficients; therefore, in the numerical implementation it is necessary to work with at least $2N$ number of samples of $f(z^2)$ in order to obtain $a_N(z^2)$ which is a polynomial of degree $N - 1$.

Finally, the input to the layer-peeling algorithm can be taken to be

$$P_1^{(N)}(z^2) = a_N(z^2), \quad P_2^{(N)}(z^2) = \check{b}_N(z^2).$$

For the TIB algorithm, we compute $\check{p}_N = \check{b}_N/a_N$ so that the discrete approximation to $p(\tau)$, which serves as the input, can be computed.

⁴ Note that the mapping $z = e^{i\zeta h}$ plays no role once $\check{b}_N(z^2)$ is determined so that one can simply speak of the variable z .

IV. NUMERICAL RESULTS

Our objective in this section is twofold: First to test the accuracy as well as complexity of the proposed methods, second, to numerically verify some of the analytical results obtained thus far. If the analytic solution is known, we quantify the error as

$$e_{\text{rel.}} = \|q^{(\text{num.})} - q\|_{L^2} / \|q\|_{L^2}, \quad (128)$$

where $q^{(\text{num.})}$ denotes the numerically computed potential and q is the exact potential. The integrals are evaluated numerically using the trapezoidal rule. When the exact solution is not known, a higher-order scheme such as the (exponential) 3-step *implicit Adams* method (IA₃) [15, 28], which has an order of convergence 4, i.e., $O(N^{-4})$, can be used to compute the accuracy of the numerical solution by computing the nonlinear Fourier spectrum using $q^{(\text{num.})}$ as the scattering potential and compare it with the known nonlinear Fourier spectrum. The error computed in this manner does not represent the *true* numerical error; therefore, the results in this case must be interpreted with caution.

A. Truncated secant-hyperbolic potential

In order to devise a test of convergence for one-sided potentials, we derive the scattering coefficients for a truncated secant-hyperbolic potential. To this end, consider $q(t) = A \operatorname{sech} t$ where $A < 0.5$ so that there are no bound states present. Let $s = \frac{1}{2}(1 - \tanh t)$, then the Jost solution $\phi(t; \zeta)$ is given by [29]

$$\begin{aligned} \phi_1 &= e^{-i\zeta t} {}_2F_1\left(A, -A; \frac{1}{2} - i\zeta; 1 - s\right), \\ \phi_2 &= -\frac{Ae^{-i\zeta t}}{\frac{1}{2} - i\zeta} \left(\frac{1}{2} \operatorname{sech} t\right) {}_2F_1\left(1 - A, 1 + A; \frac{3}{2} - i\zeta; 1 - s\right), \end{aligned}$$

where ${}_2F_1$ denotes the hypergeometric function [30]. The scattering coefficients are given by

$$\begin{aligned} a(\zeta) &= \frac{\Gamma\left(\frac{1}{2} - i\zeta\right)^2}{\Gamma\left(A + \frac{1}{2} - i\zeta\right)\Gamma\left(-A + \frac{1}{2} - i\zeta\right)}, \quad \operatorname{Im} \zeta \geq 0, \\ b(\zeta) &= -\frac{\sin(\pi A)}{\cosh(\pi \zeta)}, \quad |\operatorname{Im} \zeta| < \frac{1}{2}. \end{aligned}$$

Let $(-\infty, T]$ be the computational domain so that the truncation takes place at $t = T$ (with $s(T) = s_2$), the scattering coefficients of the left-sided potential are given by

$$\begin{aligned} a^{(-)}(\zeta) &= {}_2F_1\left(A, -A; \frac{1}{2} - i\zeta; 1 - s_2\right), \\ \check{b}^{(-)}(\zeta) &= -\frac{A \operatorname{sech} T}{2\left(\frac{1}{2} - i\zeta\right)} \cdot {}_2F_1\left(1 - A, 1 + A; \frac{3}{2} - i\zeta; 1 - s_2\right) \end{aligned}$$

Note that $s(T) \approx e^{-2T}$, therefore, we may use the asymptotic form of the hypergeometric functions to obtain the scattering

coefficients. For a -coefficient, the approximation works out to be $a^{(-)}(\zeta) = a(\zeta) + O(e^{-T(2\text{Im}(\zeta)+1)})$. For the b -coefficient, we observe that

$$\check{b}^{(-)}(\zeta) \sim Ae^{-T} \frac{a(\zeta)}{\frac{1}{2} + i\zeta} - \frac{\sin \pi A}{\cosh \pi \zeta} e^{2i\zeta T} + O(e^{-2T}), \quad (129)$$

for $\zeta \neq i(n + \frac{1}{2})$, $n = 0, 1, \dots$, and otherwise

$$\check{b}^{(-)}(\zeta) \sim \begin{cases} -\frac{2T}{\pi} e^{-T} \sin \pi A & \zeta = i/2, \\ Ae^{-T} \frac{a(\zeta)}{\frac{1}{2} + i\zeta}, & \zeta = 3i/2, 5i/2, \dots \end{cases} \quad (130)$$

in the upper half of the complex plane. For $\text{Im} \zeta = \eta > 1$, the damping term in (129), $e^{2i\zeta T} = O(e^{-2T})$; therefore

$$\check{b}^{(-)}(\zeta) \sim Ae^{-T} \frac{a(\zeta)}{\frac{1}{2} + i\zeta} + O(e^{-2T}), \quad \text{Im} \zeta > 1. \quad (131)$$

Let $\tilde{A} = A + 1/2$. For large ζ , we use the following asymptotic forms in order to evaluate $a(\zeta)$ [30]:

$$\begin{aligned} a(\zeta) &= \frac{\Gamma(-i\zeta + \frac{1}{2})}{\Gamma(-i\zeta + \tilde{A})} \left[\frac{\Gamma(-i\zeta + 1 - \tilde{A})}{\Gamma(-i\zeta + \frac{1}{2})} \right]^{-1} \sim \left(\frac{z_2}{z_1} \right)^{\tilde{A}-1/2} \\ &\times \left[1 + \frac{H_1(1/2, \tilde{A})}{z_1^2} + \frac{H_2(1/2, \tilde{A})}{z_1^4} + \dots \right] \\ &\times \left[1 + \frac{H_1(1 - \tilde{A}, 1/2)}{z_2^2} + \frac{H_2(1 - \tilde{A}, 1/2)}{z_2^4} + \dots \right]^{-1} \end{aligned}$$

where $z_1 = -i\zeta + (2\tilde{A} - 1)/4$ and $z_2 = -i\zeta + (1 - 2\tilde{A})/4$. The other constants in the expansion are defined as

$$\begin{aligned} H_1(r, s) &= -\frac{1}{12} \binom{r-s}{2} (r-s+1), \\ H_2(r, s) &= \frac{1}{240} \binom{r-s}{4} [2(r-s+1) + 5(r-s+1)^2]. \end{aligned}$$

The truncation point $t = T$ is chosen large enough so that the reflection coefficient $\rho^{(-)}(\xi)$ becomes effectively a Schwartz class function. This would allow us to test for the following algorithms:

- LP_ρ^* : This refers to the layer-peeling algorithm where the input is synthesized using complex integration in the upper half of the complex plane as described in Sec. III A 2. For simplicity, we may also refer to it as the Lubich method.
- LP_ρ : This refers to the layer-peeling algorithm where the input is synthesized using the discrete approximation of the Fourier integral as Sec. III A 2.
- LP_b : This refers to the layer-peeling algorithm where the input is synthesized using the b -coefficient as described in Sec. III C.
- **TIB**: This refers to the second order TIB algorithm reported in [16, 17].

- **TIB***: This refers to the modified second order TIB algorithm presented in Sec. III B.

The over sampling factor for synthesizing the input is taken to be $n_{\text{os}} = 8$. This means that for Cauchy or the Fourier integral, the number of samples of $\rho^{(-)}(\zeta)$ used is $M = 8N$ where $N \in \{2^{10}, 2^{11}, \dots, 2^{20}\}$.

For the first test, we set $A_R = 0.4$. The results of the convergence and complexity analysis are plotted in Fig. 1. The results show that all the methods exhibit a second order of convergence. The Lubich method where complex integration is employed turns out to be the least accurate. The TIB and TIB* show small difference in accuracy. The plot depicting the total run-time per sample shows linear growth for TIB and TIB* with respect to $\log N$ while the others exhibit a logarithmic growth. Therefore, the layer-peeling algorithm is an order of magnitude faster than the integral method.

For the second test, we set $A_R = 0.5 - \delta$ where $\delta \in \{10^{-2}, 10^{-4}, 10^{-6}, 10^{-8}\}$. From the analytic solution, it is evident that as the value of δ decreases, a pole in \mathbb{C}_- approaches the real axis. This makes it a challenging test case for methods that sample $\rho^{(-)}(\zeta)$ on the real axis on account of the numerical ill-conditioning introduced by the proximity of the pole to the real axis. The results of the convergence analysis are plotted in Fig. 2 where all methods tend to fail except for LP_ρ^* , the Lubich method. The unusual stability of this method is attributed to the fact that samples of $\rho^{(-)}(\zeta)$ is sought in \mathbb{C}_+ avoiding any ill-conditioning introduced as a result of the proximity of the pole in \mathbb{C}_- to the real axis.

B. Raised-cosine filter

In this test case, we consider generation of time-limited signals using a b -coefficient that is an entire function of exponential type. Let $\Omega_h = [-\pi/2h, \pi/2h]$, then the error is quantified by

$$e_{\text{rel.}} = \|\rho^{(\text{num.})} - \rho\|_{L^2(\Omega_h)} / \|\rho\|_{L^2(\Omega_h)}, \quad (132)$$

where the integrals are computed from N equispaced samples in Ω_h using the trapezoidal rule. The quantity $\rho^{(\text{num.})}$ is computed using the (exponential) IA₃.

Let us define

$$f_{\text{rc}}(\xi) = A_{\text{rc}} \text{sinc} [2(1 - \chi)\xi T] \frac{\cos(2\chi\xi T)}{1 - \left(\frac{4\chi\xi T}{\pi}\right)^2}, \quad (133)$$

which is a representation of the raised-cosine filter (in the ‘‘time’’ domain). We set $A_{\text{rc}} = 0.489$, $\chi = 0.3$ and $T = 1$ so that the support of the potential works out to be $[-T, T]$. We then synthesize b as follows:

$$b(\xi) = \sum_{n \in J} c_n f_{\text{rc}}(\xi - \xi_n) \quad (134)$$

where $c_n \in \{-1, +1\}$ is chosen randomly and $\xi_n = (2\pi/4T)n$. The index set is defined as $J = \{-N_{\text{sym}}/2, \dots, N_{\text{sym}}/2 - 1\}$ with $N_{\text{sym}} \in \{16, 32, \dots, 2048\}$. Here, we would conduct numerical

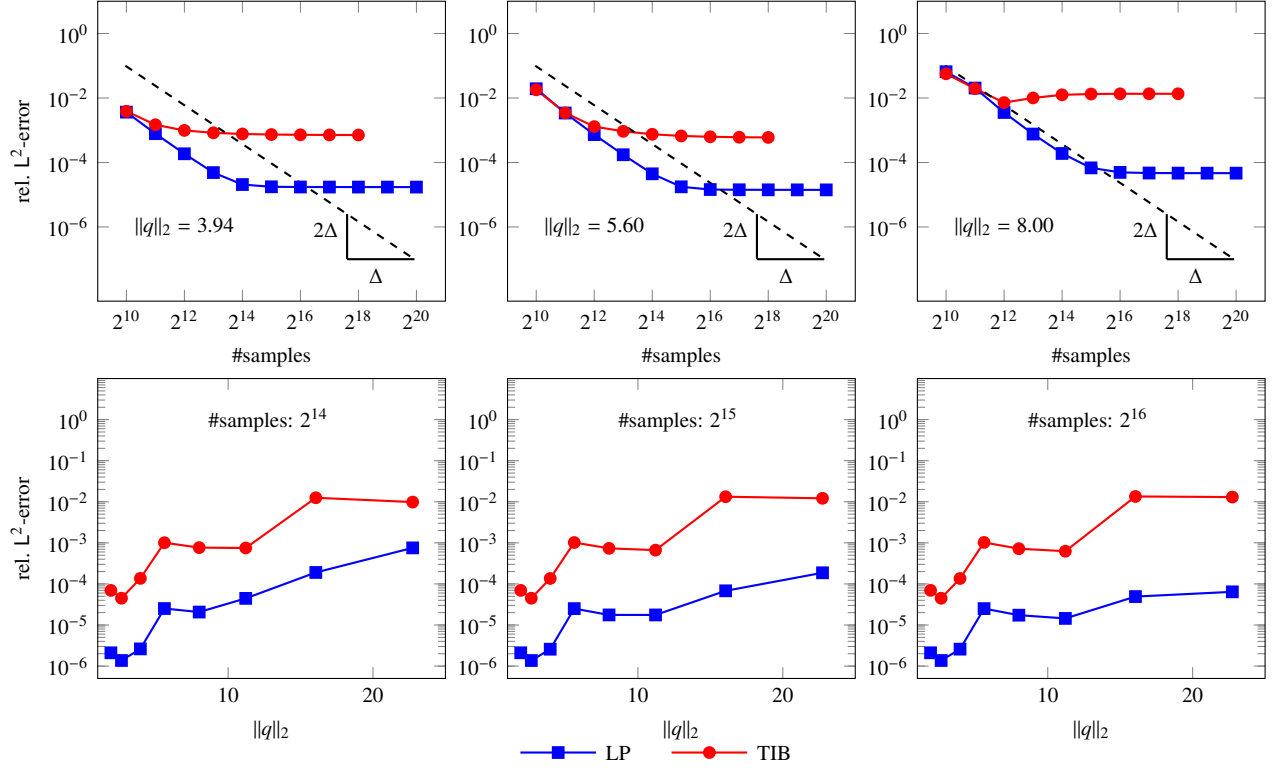


FIG. 3. The figure shows the error analysis for the signal generated from the b -coefficient given by (134). The error is quantified by (132).

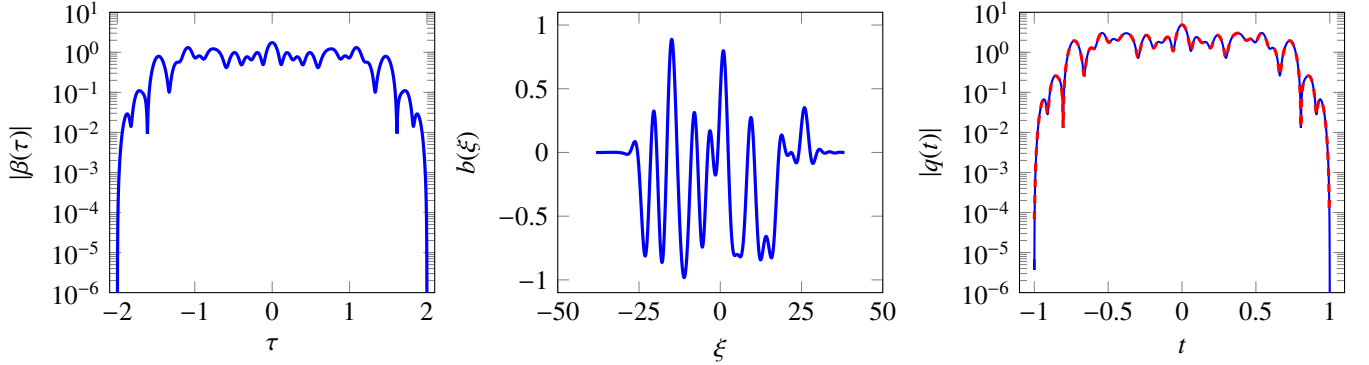


FIG. 4. The figure shows an example of synthesized time-limited signal from a compactly supported $\beta(\tau)$ or a b -coefficient that is of exponential type. Here $N_{\text{sym}} = 32$ and $\|q\|_2 = 2.64$. In the last plot the solid and the dashed lines correspond to the potential computed using the LP and the TIB algorithm, respectively.

experiments with varying number of samples and fixed N_{sym} or with different values N_{sym} and fixed N . In these experiments, we compare the LP algorithm to the TIB algorithm presented in Sec. III B. The input to both of these algorithms is synthesized from the b -coefficient as discussed in Sec. III C.

The results of the error analysis are displayed in Fig. 3. The plots in the top row indicate that the error as a function of N shows a second order slope before it plateaus after a certain value. This plateauing does *not* necessarily indicate the lack of convergence because the error does not represent the true numerical error. Further, it is evident from these plots that the

error for TIB algorithm plateaus much earlier than that of the LP algorithm; therefore, the LP algorithm is superior to TIB in terms of accuracy. The same conclusion about the accuracy of LP as compared to TIB can be drawn from the plots in the bottom row where the error is plotted as a function of the L^2 -norm of the potential which is the result of varying N_{sym} .

The specific examples of the signals generated with $N = 2^{12}$ for $N_{\text{sym}} = 32, 64, 128$ are displayed in figures 4, 5 and 6, respectively. The generated signal shows the correct decay behavior such that the compact support of the potential can be inferred easily.

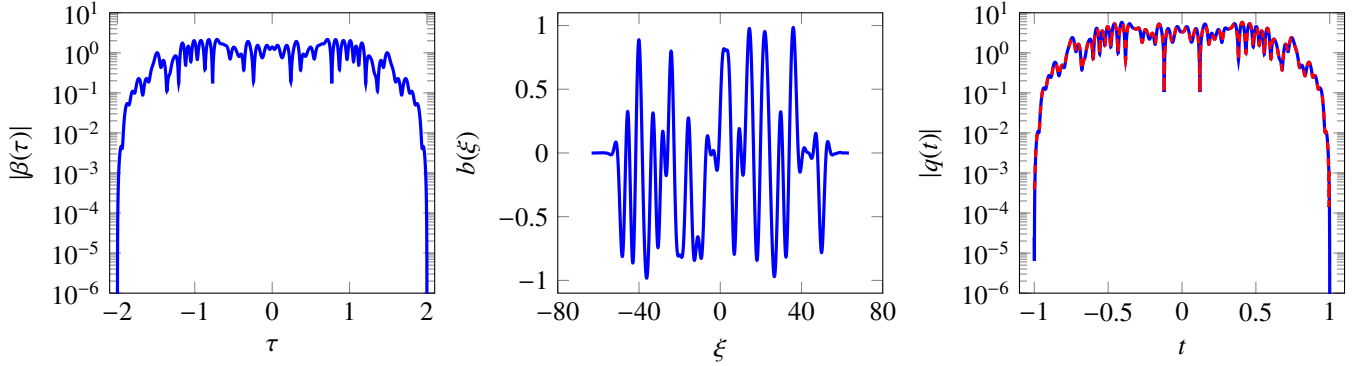


FIG. 5. The figure shows an example of synthesized time-limited signal from a compactly supported $\beta(\tau)$ or a b -coefficient that is of exponential type. Here $N_{\text{sym}} = 64$ and $\|q\|_2 = 3.94$. In the last plot the solid and the dashed lines correspond to the potential computed using the LP and the TIB algorithm, respectively.

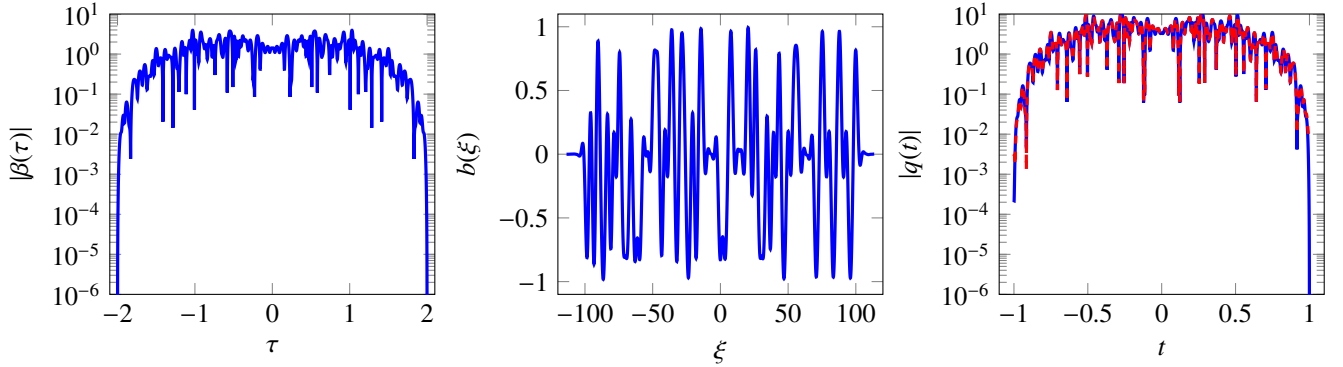


FIG. 6. The figure shows an example of synthesized time-limited signal from a compactly supported $\beta(\tau)$ or a b -coefficient that is of exponential type. Here $N_{\text{sym}} = 128$ and $\|q\|_2 = 5.6$. In the last plot the solid and the dashed lines correspond to the potential computed using the LP and the TIB algorithm, respectively.

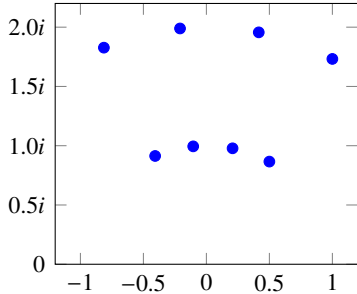


FIG. 7. The figure shows the eigenvalues to be ‘added’ to the compactly supported potential generated using the b -coefficient.

The final test that we consider has to do with the addition of bound states to compactly supported potentials. The signal is generated using the fast Darboux transformation algorithm (FDT) reported in [14]. Define

$$\theta = (\pi/3, 13\pi/30, 8\pi/15, 19\pi/30) \quad (135)$$

and let the set of eigenvalues be $\{\exp(i\theta), 2\exp(i\theta)\}$ (see

Fig. 7). The norming constants are chosen such that the resulting potential is supported on $(-\infty, 1]$, i.e., $b_k = b(\zeta_k)$. The specific examples of the signals are generated with $N = 2^{12}, 2^{14}$ for $N_{\text{sym}} = 32, 64, 128$ are displayed in Fig. 8. The generated signal shows a non-zero tail beyond $t = 1$ which can be attributed to the numerical errors. The tail, however, becomes less significant as the number of samples is increased from $N = 2^{12}$ to $N = 2^{14}$.

V. CONCLUSION

To conclude, we have presented some useful regularity properties of the nonlinear Fourier spectrum under various assumptions on the scattering potential. These results bear a close resemblance to the Paley-Wiener theorems for Fourier-Laplace transform. We have further provided the necessary and sufficient conditions for the nonlinear Fourier spectrum such that the corresponding scattering potential has a prescribed support. In addition, we also analyzed how to exploit the regularity properties of the scattering coefficients to im-

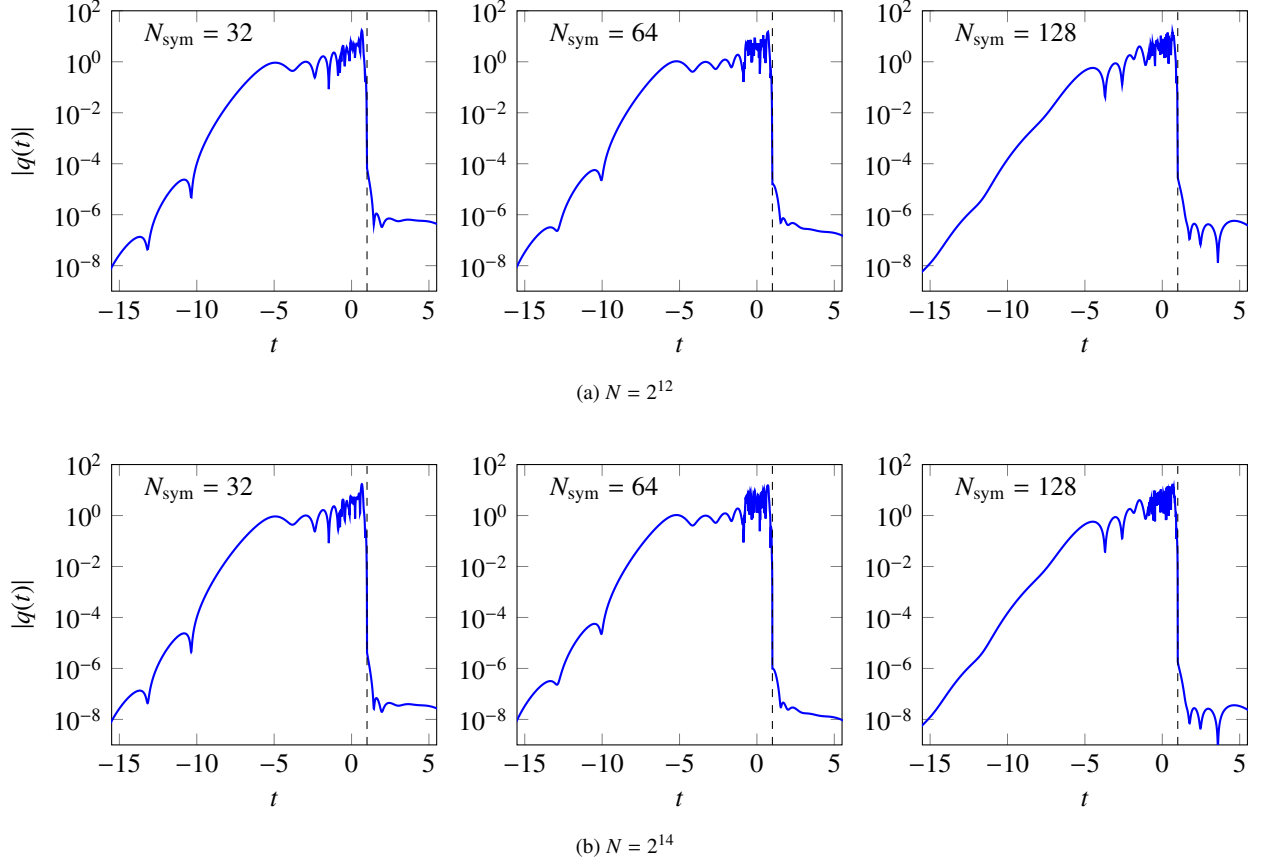


FIG. 8. The figure shows the signal generated using the b -coefficient given by (134) and the eigenvalues shown in Fig. 7. The norming constants are chosen such that the signal is supported in $(-\infty, 1]$. It is evident that increasing the number of samples (N) tends to make the tail beyond $t = 1$ (marked by the vertical dashed line) less significant.

prove the numerical conditioning of the differential approach of inverse scattering. For the sake of comparison, we considered the integral approach originally presented in [16, 17] and provided the correct derivation of the so called Töplitz inner-bordering scheme. The comparative study of the two approaches conducted in the article clearly reveals that the differential approach is more accurate while admittedly being faster by an order of magnitude for the class of nonlinear Fourier spectra considered in this article.

Appendix A: Proof of Lemma II.2

The proof is almost similar to that of the Riemann-Lebesgue lemma [19, Chap. 13]. First, we note that

$$|\Phi_2(t; \zeta)| \leq \int_{-T_-}^t |q(y)| e^{-2\eta(t-y)} dy \leq \max(1, e^{-2\eta W}) \|q\|_{L^1},$$

where $W = T_- + T_+$. Let $\tau = \pi\xi/(2|\xi|^2)$ and consider the case $\eta = 0$: From the relation

$$\begin{aligned} \int_{-\infty}^t r(y + \tau) e^{2i\xi(t-y)} dy &= - \int_{-\infty}^{t+\tau} r(u) e^{2i\xi(t-u)} du \\ &= -\Phi_2(t; \xi) - \int_t^{t+\tau} r(u) e^{2i\xi(t-u)} du, \end{aligned}$$

we may write

$$2|\Phi_2(t; \xi)| \leq \int_{-\infty}^{T_+} |q(y) - q(y + \tau)| dy + \int_t^{t+\tau} |q(y)| dy. \quad (\text{A1})$$

Now, as $|\xi| \rightarrow \infty$, we have $\tau \rightarrow 0$ so that, using the continuity of translation for L^1 -functions [19, Chap. 7], we conclude that the first term on the right hand side of above tends to zero. The second term can be shown to approach the limit 0 uniformly as $\tau \rightarrow 0$ on account of the theorem on absolute continuity [19, Chap. 6]. Therefore, we conclude $|\Phi_2(t; \xi)| \rightarrow 0$ uniformly in Ω as $|\xi| \rightarrow \infty$. For fixed $\eta > 0$, we have

$$\begin{aligned} |\Phi_2(t; \xi + i\eta)| &\leq \frac{1}{1 + e^{-2\eta\tau}} \int_{-\infty}^{T_+} |q(y) - q(y + \tau)| dy \\ &\quad + \left(\frac{1 - e^{-2\eta\tau}}{1 + e^{-2\eta\tau}} \right) \|q\|_{L^1} + \frac{e^{-2\eta\tau}}{1 + e^{-2\eta\tau}} \int_t^{t+\tau} |q(y)| dy. \end{aligned}$$

Therefore, we conclude that, for fixed $\eta \geq 0$, $|\Phi_2(t; \xi + i\eta)| \rightarrow 0$ uniformly in Ω as $|\xi| \rightarrow \infty$.

Now, consider $\zeta = \xi - i\eta$ where $\eta > 0$ is fixed such that $\eta < \infty$. It is straightforward to show that

$$|\Phi_2(t; \xi - i\eta)| \leq \frac{e^{2\eta W}}{1 + e^{2\eta\tau}} \int_{-\infty}^{T_+} |q(y) - q(y + \tau)| dy + \left(\frac{1 - e^{-2\eta\tau}}{1 + e^{-2\eta\tau}} \right) e^{2\eta W} \|q\|_{L^1} + \frac{e^{2\eta W}}{1 + e^{2\eta\tau}} \int_t^{t+\tau} |q(y)| dy.$$

Therefore, we can again show that $|\Phi_2(t; \xi - i\eta)| \rightarrow 0$ uniformly for $t \in \Omega$ as $|\xi| \rightarrow \infty$.

Finally, combining the results obtained above, we have

$$\lim_{|\xi| \rightarrow \infty} \|\Phi_2(t; \xi + i\eta)\|_{L^\infty(\Omega)} = 0,$$

for fixed $\eta \in \mathbb{R}$ and $\eta < \infty$.

Appendix B: Proof of Lemma II.5

In the following, we assume that the functions F and G are redefined appropriately so that factors of the form $e^{-2i\zeta T}$ are no longer present. Therefore, we prove the lemma for the case $T = 0$.

Observing that $F(\xi + i\eta)$, as a function of $\xi \in \mathbb{R}$, is in L^2 for $\eta \geq 0$, it is evident that $f(\tau) \in L^2$ and it is supported in $\Omega = [0, \infty)$. Using Cauchy's estimate taken on the disc $\{\zeta' \in \mathbb{C}_+ : |\zeta' - (\xi + i\eta)| \leq \eta/2, \eta > 0\}$, we have

$$|F'(\xi + i\eta)| \leq \frac{2C}{\eta(1 + |\xi + i\eta| - \eta/2)}, \quad \eta > 0,$$

therefore, $F'(\xi + i\eta)$, as a function of $\xi \in \mathbb{R}$, is in L^2 for $\eta > 0$. From Paley-Wiener theorem, we know that the boundary function $\lim_{\eta \rightarrow 0} F'(\xi + i\eta)$ exists (which coincides with $F'(\xi)$ in this case) and it belongs to L^2 . From Cauchy-Schwartz inequality [19, Chap. 10], we have

$$\left| \int_{\Omega} \sqrt{1 + \tau^2} f(\tau) \cdot \frac{d\tau}{\sqrt{1 + \tau^2}} \right|^2 \leq \frac{\pi}{2} \int_{\Omega} (1 + \tau^2) |f(\tau)|^2 d\tau,$$

so that $\|f\|_1 \leq (1/4)(\|F(\xi)\|_2^2 + \|F'(\xi)\|_2^2)$. The last step follows from Plancherel's theorem [19, Chap. 13]. Therefore, we conclude that $f(\tau) \in L^1 \cap L^2$.

Next, under the assumption of part (b), we would like to show that $f(\tau)$ is absolutely continuous in $[0, \infty)$, i.e., there exists a complex-valued function $f^{(1)}(\tau)$ such that

$$f(\tau) = f(0+) + \int_0^\tau f^{(1)}(\tau') d\tau', \quad \tau \in \Omega. \quad (\text{B1})$$

Let us observe the property

$$\int_0^\infty \left[\int_0^\tau f^{(1)}(\tau') d\tau' \right] e^{i\zeta\tau} d\tau = -\frac{1}{i\zeta} \int_0^\infty f^{(1)}(\tau) e^{i\zeta\tau} d\tau.$$

Note that $g(\tau) \in L^1 \cap L^2$ since $G(\zeta)$ satisfies the same kind of estimate as that of $F(\zeta)$. The relation (B1) then follows by noting that $G(\zeta)/(-i\zeta)$ is the Fourier-Laplace transform of $\int_0^\tau g(\tau') d\tau'$ and $G(\zeta)/i\zeta = F(\zeta) - \mu/i\zeta$; therefore, $f^{(1)}(\tau) = g(\tau)$. Absolute continuity of $f(\tau)$ also implies continuity of $f(\tau)$ over $[0, \infty)$; consequently, the limit $f(0-)$ exists and equals μ . Finally, using the Lebesgue's theorem [19, Chap. 16] on differentiation, we have $\partial_\tau f(\tau) = g(\tau)$ almost everywhere. It also follows that $|f(\tau)| \leq |\mu| + \|g\|_1$, i.e., $f(\tau)$ is bounded on $[0, \infty)$.

-
- [1] V. E. Zakharov and A. B. Shabat, Sov. Phys. JETP **34**, 62 (1972).
 - [2] M. J. Ablowitz, D. J. Kaup, A. C. Newell, and H. Segur, Stud. Appl. Math. **53**, 249 (1974).
 - [3] M. Ablowitz and H. Segur, *Solitons and the Inverse Scattering Transform* (Society for Industrial and Applied Mathematics, Philadelphia, 1981).
 - [4] Y. Kodama and A. Hasegawa, IEEE J. Quantum Electron. **23**, 510 (1987).
 - [5] G. P. Agrawal, *Nonlinear Fiber Optics*, 3rd ed., Optics and Photonics (Academic Press, New York, 2013).
 - [6] S. K. Turitsyn, J. E. Prilepsky, S. T. Le, S. Wahls, L. L. Frumin, M. Kamalian, and S. A. Derevyanko, Optica **4**, 307 (2017).
 - [7] R. Fedec and M. N. Zervas, J. Opt. Soc. Am. A **17**, 1573 (2000).
 - [8] J. K. Brenne and J. Skaar, J. Lightwave Technol. **21**, 254 (2003).
 - [9] V. Vaibhav, Commun. Nonlinear Sci. Numer. Simul. **61**, 22 (2018).
 - [10] G. L. Lamb, *Elements of soliton theory*, Pure and applied mathematics (John Wiley & Sons, Inc., New York, 1980).
 - [11] D. E. Rourke and P. G. Morris, Phys. Rev. A **46**, 3631 (1992).
 - [12] D. E. Rourke and J. K. Saunders, J. Math. Phys. **35**, 848 (1994).
 - [13] H. Steudel and D. J. Kaup, Inverse Probl. **24**, 025015 (2008).
 - [14] V. Vaibhav, Phys. Rev. E **96**, 063302 (2017).
 - [15] V. Vaibhav, Phys. Rev. E **98**, 013304 (2018).
 - [16] O. V. Belai, L. L. Frumin, E. V. Podivilov, and D. A. Shapiro, J. Opt. Soc. Am. B **24**, 1451 (2007).
 - [17] L. L. Frumin, O. V. Belai, E. V. Podivilov, and D. A. Shapiro, J. Opt. Soc. Am. B **32**, 290 (2015).
 - [18] G. Gripenberg, S. O. Londen, and O. Staffans, *Volterra Integral and Functional Equations*, Encyclopedia of Mathematics and Its Applications, Vol. 34 (Cambridge University Press, Cambridge, 1990).
 - [19] F. Jones, *Lebesgue Integration on Euclidean Space*, Jones and Bartlett books in mathematics (Jones and Bartlett, Massachusetts, 2001).
 - [20] K. Yosida, *Functional Analysis*, 2nd ed., Die Grundlehren der mathematischen Wissenschaften (Springer, Berlin, 1995).
 - [21] R. P. Boas, *Entire Functions*, Pure and Applied Mathematics (Academic Press Inc., New York, 1954).
 - [22] C. L. Epstein, J. Magn. Reson. **167**, 185 (2004).
 - [23] C. Gu, A. Hu, and Z. Zhou, *Darboux Transformations in Integrable Systems: Theory and their Applications to Geometry*, Mathematical Physics Studies (Springer, Netherlands, 2005).
 - [24] J. Lin, Acta Mathematicae Applicatae Sinica **6**, 308 (1990).
 - [25] C. Lubich, Numer. Math. **52**, 129 (1988).
 - [26] C. Lubich, Numer. Math. **67**, 365 (1994).

- [27] P. Henrici, *Applied and Computational Complex Analysis, Volume 3: Discrete Fourier Analysis, Cauchy Integrals, Construction of Conformal Maps, Univalent Functions*, Applied and Computational Complex Analysis (John Wiley & Sons, Inc., New York, 1993).
- [28] V. Vaibhav, *IEEE Photonics Technol. Lett.* **30**, 700 (2018).
- [29] J. Satsuma and N. Yajima, *Prog. Theor. Phys. Suppl.* **55**, 284 (1974).
- [30] F. W. J. Olver, D. W. Lozier, R. F. Boisvert, and C. W. Clark, eds., *NIST Handbook of Mathematical Functions* (Cambridge University Press, New York, 2010).